Journal of Archaeological Science, Volume 123, November 2020, Article number 105220
DOI:10.1016/j.jas.2020.105220

Direct Evidence for the Co-Manufacturing of Early Iron and Copper-Alloy Artifacts in the Caucasus

Nathaniel L. Erb-Satullo[1]

Dimitri Jachvliani[2]

Kakha Kakhiani[2]

Richard Newman[3]

[1] Research Lab for Archaeology and the History of Art, School of Archaeology, 1 South Parks Rd, Oxford OX1 3TG, United Kingdom; nathaniel.erb-satullo@arch.ox.ac.uk; corresponding author.

[2] Otar Lordkipanidze Archaeology Institute, Georgian National Museum, 3 Rustaveli Avenue 0105 Tbilisi, Georgia

[3]Scientific Research Laboratory, Museum of Fine Arts, Boston, 465 Huntington Ave, Boston, MA, 02115

Abstract

Models for iron innovation in Eurasia are predicated on understanding the relationship between the bronze and iron industries. In eastern Anatolia, South Caucasus, and Iran, the absence of scientific analyses of metallurgical debris has obscured the relative chronology, spatial organization, and economic context of early iron and contemporary copper-alloy industries. Excavation and surface survey at Mtsvane Gora, a fortified hilltop site close to major polymetallic ore sources in the Lesser Caucasus range, recovered metallurgical debris dating to the 8th-6th centuries BC. Optical microscopy, scanning electron microscopy, and energy and wavelength dispersive spectrometry revealed evidence for both iron and copper-alloy metallurgy, including smithing and alloying. Metal particles trapped within clear iron smithing slags were contaminated with copper, arsenic, and tin, suggesting that iron and copper-alloy working took place in the same hearths. The discovery of a small fragment of unprocessed material consisting of pyrite and jarosite, minerals typical of major nearby polymetallic ore deposits, links the secondary smithing and alloying at Mtsvane Gora with nearby mining activities, though the nature of those connections remains unclear. While the earliest iron in the region probably predates the Mtsvane Gora assemblage, the remains date to a period when iron use was still expanding, and they are at present the earliest analytically confirmed, radiocarbon-dated iron metallurgical debris in the Caucasus. The remains are therefore significant for understanding the spread of iron innovation eastward from Anatolia and the Levant. When considered in light of evidence from other Near Eastern sites, the results support a model for innovation in which early iron manufacturing was at least partially integrated with the copper-alloy metallurgical economy.

Keywords: slag; smithing; metallurgy; innovation; adoption; technology; Georgia

Introduction

The adoption of iron metallurgy was a major technological transformation in pre- and proto-historic Eurasia, though one whose societal impact, at least initially, may have been somewhat muted. While meteoritic iron was used for artifacts since about 3000 BC and smelted iron possibly as early as 2000 BC (Erb-Satullo, 2019:562-566; Johnson, et al., 2013; Rehren, et al., 2013), significant increases in iron use in the core regions of Anatolia and the Levant occurred in the late 2nd and early 1st millennium BC (Gottlieb, 2010; McClellan, 1975:738; Yahalom-Mack and Eliyahu-Behar, 2015). By 500 BC, iron use had spread across a large swath of Eurasia. Possible explanations for this transformation include both technical factors, such as the development of reliable and consistent iron smelting techniques, as well as socio-political factors, such as the desire to develop local supplies of metal (Erb-Satullo, 2019). However, the narrative of iron innovation in the Near East is largely written from the perspective of the Levant and adjacent regions. The overwhelming majority of research on Late Bronze and Early Iron Age metal production focuses on eastern Mediterranean, with models of iron innovation primarily based on conditions specific to these areas. The attention this region has received is well justified, but the social, cultural, and environmental context of early iron-using societies in other areas of the Near East, including the South Caucasus and Iran, differs significantly. One cannot assume Levantine models for iron innovation apply equally across the Near East.

Given its proximity to Anatolia, a probable center of early iron innovation, the Caucasus is key for understanding the spread of iron north and east into the heartland of Eurasia. If the idea of iron metallurgy spread from the from west to east across Eurasia, it did so quite rapidly, with iron use appearing in East Asia even as it was still being established in part of the Near East (compare Erb-Satullo, 2019:574; Lam, 2014:519). This process of Eurasian adoption cannot be explained without understanding the role of regions like Iran, the Caucasus, and the areas around the Black Sea. Yet, while numerous early iron artifacts have been found in the Caucasus region, the question of iron production—its chronology, its social context, and its relationship with contemporary bronze production industries—remains unclear. Recent reevaluations of alleged early iron smelting sites in western Georgia have meant that there are virtually no well-dated, analytically-confirmed iron metallurgical sites in the Caucasus or Iran before 500 BC (Erb-Satullo, et al., 2014). The lack of information about the eastward spread of iron innovation

contrasts to the more robust understanding of the spread of iron metallurgy westward across the Mediterranean (e.g. Kaufman, et al., 2016; Renzi, et al., 2013; Snodgrass, 1980).

The discovery of metallurgical debris at a late 2nd and early 1st millennium BC fortified hilltop site called Mtsvane Gora has the potential to reveal the context and organization of metal production during the crucial period when iron spread across Eurasia. Surface survey and targeted excavation were used to explore the chronology and context of metallurgical activities at the site, while chemical and microscopic analysis reconstructed technological and organizational aspects of production, including the type of metals worked, the stages of production, and the spatial connections between different metallurgical activities.

Analysis of metallurgical debris from Mtsvane Gora has implications for the relationship between bronze and iron industries. In regions like the Caucasus, where early iron objects closely mimic contemporary bronzes, are bronze and iron objects made in the same workshops by the same craftspeople? Or, alternatively, are they the products of specialized ironworkers competing with bronzeworkers to produce objects that appeal to pre-existing consumer sensibilities? Existing evidence is equivocal. On one hand, there are several cases in the Levant where iron and copper metallurgical debris have been found together (Eliyahu-Behar, et al., 2012; Erb-Satullo and Walton, 2017; Roames, 2011). On the other hand, there have been no unequivocal examples of iron and copper smelting (i.e. the reduction of ore to metal) at the same sites, despite much speculation and discussion about the possible invention of iron smelting during the process of copper smelting (Erb-Satullo, 2019:574-576; Gale, et al., 1990; Merkel and Barrett, 2000). Furthermore, some Anatolian texts name iron and copper-alloy workers separately as early as the mid-second millennium BC, perhaps hinting at specialization of craftspeople by metal type (Cordani, 2016:171-172). Analysis of workshops and production debris provides direct evidence for the spatial organization and technical processes carried out by metalworkers.

Iron Innovation in the Caucasus

The South Caucasus (**figure 1**) is in a key position for understanding the diffusion of iron technologies to the north and east from Anatolia and the Levant into the Eurasian Steppes and Central Asia. Investigations of iron innovation in Eastern Anatolia and the South Caucasus face significant challenges. There have been several admirable attempts at synthesis (Çifçi, 2017;

McConchie, 2004; Nieling, 2009), but it is worth stressing that these reviews rely in part on assemblages that have not been dated by radiometric methods, or on field identifications of metallurgical debris that have not been verified through scientific analysis. In eastern Anatolia and the South Caucasus, Late Bronze and Early Iron Age ceramic assemblages are notoriously similar, confounding efforts to build a detailed chronology of iron adoption. Modern political boundaries make correlating data across different countries, each with their local archaeological traditions, particularly difficult (Çevik, 2008). Correct identification of metallurgical remains is fundamentally important to tracking iron innovation, but cases of misidentification have seriously hampered these efforts (Erb-Satullo, et al., 2014; Erb-Satullo, 2018).

Taking these caveats into consideration, it is nevertheless possible to sketch the broad outlines of technological transformation, albeit with some degree of chronological imprecision. In eastern Anatolia, numerous iron objects are found in cemeteries at Karagündüz, Yoncatepe, and other sites in the Van area, with radiocarbon dates in the 1200-800 BC range. The high proportion of iron relative to bronze in these tombs has led some to suggest an earlier adoption in eastern Anatolia relative to the South Caucasus (Çevik, 2008:10). However, the chronology of these sites is contentious, as some have dated them to the Urartian period (c. 900-600 BC) (Köruoğlu and Konyar, 2008). In present day Armenia and Eastern Georgia, iron artifacts are reported from late 2nd millennium graves (Abramishvili, 1957; Khanzadian, 1995:67), but radiocarbon dates are lacking. In the western Caucasus, along the Black Sea coast, iron artifacts appear in large quantities from the 8th-7th centuries BC, but initial adoption seems to be slightly later than in the middle Kura and Araxes river valleys (Abramishvili, 1957; Japaridze, 1999; Papuashvili, 2011). In northwestern Iran, iron artifacts are rare before the 11th century BC, but the late 9th century BC destruction layer at Hasanlu contains large quantities of iron metal (Danti, 2013:348, 356-359). In sum, the record of iron artefacts suggests that, although the beginnings of iron adoption may be tentatively located in the late 2nd millennium BC, it is not until the first half of the 1st millennium BC that iron achieved widespread adoption.

Direct evidence for iron metallurgical activities, as opposed to finished artifacts, is more limited. Soviet-period research suggested very early dates for iron smelting sites in the Black Sea area (Khakhutaishvili, 1987), but more recent work has shown them to be copper smelting sites (Erb-Satullo, et al., 2014; Erb-Satullo, et al., 2015). At present, the earliest well-documented iron smelting remains in the Black Sea area date to the mid-late 1st millennium BC (Erb-Satullo, et

al., 2020a). Reports of iron metallurgical debris are documented in other areas of the South Caucasus (Badaljan, et al., 1993:17; Gzelishvili, 1964:31-38; Maddin, 1975; Martirosyan, 1974:97), but none have combined robust radiometric dating with scientific analyses of the metallurgical debris. Similarly, there are reports of significant slag mounds in the Lake Van region that might date to the Iron Age, but their chronology and even their identification as iron smelting slags remains largely unproven (Belli, 1991; Burney, 1996:6; Çifçi, 2017:120). Against the background of prior research, the discovery of metallurgical debris at Mtsvane Gora provides much needed data on the chronology and context of early iron metallurgy in the Caucasus.

Survey and Excavation at Mtsvane Gora

Due to the major ore zones on both sides of the Georgian-Armenian border, the area around Mtsvane Gora has a long history of metal production, though recent archaeological research has tended to focus on earlier periods (Stöllner and Gambashidze, 2011; Stöllner and Gambashidze, 2014). The site is situated on a prominent hill overlooking a major route of travel between the Kura River Valley and Lesser Caucasus highlands (**figure 1**). The hilltop was fortified with an encircling wall that is clearly visible on both aerial photographs and digital slope models (Erb-Satullo, et al., 2019).

Metal production debris in association with Late Bronze and Early Iron Age pottery was discovered during the initial survey of the site. All samples of slag identified on the surface of the site were collected, including those found outside the systematic surface collection grids (**figure 2**) (Erb-Satullo, 2018). The quantity of surface-collected slag and other metallurgical debris was small in comparison with contemporary South Caucasus smelting sites, which frequently contain tons of debris (cf. Erb-Satullo, et al., 2017), and a magnetometry survey failed to identify any major buried concentrations of the slag (Erb-Satullo, et al., 2019). Either the bulk of the debris was disposed of off the hill, or, more likely, the metallurgical activities did not produce large quantities of slag.

Several trenches were excavated just upslope from a surface concentration of slag in order to obtain metallurgical remains from stratified, well-dated deposits. The steep slope, erosion, and occasional bioturbation negatively impacted the preservation of buried deposits. Nevertheless, careful excavation recovered a stratigraphic sequence containing metallurgical

184 debris in Trench 1. The earliest phase of occupation consisted of a beaten clay floor directly
185 abutting the interior of the fortification wall. The floor was covered with an assemblage of flat-
186 lying ceramics with many joining sherds, animal bones, and stone implements (**figure 3**). A
187 possible post base and a poorly preserved stone wall running perpendicular to the encircling
188 fortification wall were identified. Despite the poor architectural preservation, the floor
189 assemblage itself was well preserved, with many large joining sherds and some nearly complete
190 vessels lying directly on it. Two charcoal samples taken from different places on the floor gave
191 almost identical readings, with 2σ date ranges in the 14th-13th century BC (**table 1**). While there
192 were some concentrations of ashy material, no unequivocal metallurgical debris was found
193 directly on this earlier floor surface.
194 Overlying the floor surface was a series of soft ashy deposits with occasional flat patches
195 of clay. Two radiocarbon dates from these overlying deposits yielded dates in the 2nd quarter of
196 the 1st millennium BC. Ceramics in this phase are broadly similar to those of the earlier phase,
197 and the character of the pottery, which differs from the mid-7th to late-4th c. BC ceramic
198 assemblage at Tsaghkahovit (Khatchadourian, 2018), tentatively favors an earlier date within the
199 broader radiocarbon range: the 8th-7th century BC rather than the 6th century BC. These
200 overlying deposits contained pieces of metallurgical debris, including fragments of dense slag
201 cakes, a smaller dribble of dense slag, and small pieces of light vitrified, vesicular slags. Due to
202 its association with the other clear metallurgical debris, this last category of debris is almost
203 certainly also metallurgical in origin. In addition, microscopic flakes of hammerscale—a product
204 of iron smithing—were recovered from sediment samples taken from these contexts. These slag
205 deposits were not associated with a well-preserved floor level, though patches of clay and short
206 linear stone alignments were noted during excavation. Nevertheless, it is highly likely that the
207 metallurgical workspaces were located within the fortification wall, as natural erosion would
208 only move debris downhill, and there is little reason for metalworkers to climb a hill to dumb
209 metallurgical debris. While colluvial erosion, and in places animal burrowing disturbed these
210 upper deposits, these processes most likely did not introduce post-LBA-EIA material, for the
211 simple reason that the site had no significant later occupation. Only two clearly Medieval glazed
212 sherds were recovered from either surface collection and excavation, and both were found on the
213 north side of the hill, well away from the deposits in question. Overall, the stratigraphy,

ceramics, and radiocarbon dates from the excavations constrained the age of the metallurgical debris to the 8th-6th century BC, with the ceramics suggesting an earlier date within that range.

Materials and Methods

Several types of metallurgical debris were recovered from excavation and surface collection. Fragments of dense slag were recovered from both excavated contexts and surface collection. Larger pieces often formed plano-convex or concavo-convex slag cakes roughly 8-10 cm in diameter (**figure 4**). The morphology of these slag cakes strongly suggests that they are smithing hearth bottoms, which forms from flakes of oxidized iron and slag which fall into the smithing hearth. A small dribble of dense slag was also identified in the same context as the two 8th-6th c. BC radiocarbon dates. The only macroscopic evidence of copper-working at the site was a slagged technical ceramic rim fragment with barely visible traces of green copper corrosion. A small fragment of a tuyère with a slagged tip was also found on the surface of the site. The complete bore-hole was not preserved, but it was estimated to be about 12 mm, narrower than those of LBA-EIA copper smelting tuyères from Western Georgia. A piece of crumbly yellow mineral with brassy yellow inclusions was also recovered during excavation.

Another class of debris includes pieces of vitrified or partially vitrified material. Some fragments have the appearance of partly melted rock fragments, while other more fully vitrified samples have vesicular textures with bloating pores. Some such pieces were very small (<1 cm), and they are less dense than the smithing hearth bottom slags. Their association with the dense cakes and cake fragments reliably links them with the metallurgical activities, and they were preliminarily interpreted as vitrified hearth materials and/or fuel ash.

Other artifacts found at the site may be associated with metallurgical activities, but with less certainty. Stone implements, including possible hammering and grinding/abrading tools were found in significant quantities, and may have been used for smithing. Most hammerstones were rounded river cobbles clearly out of place on a hilltop; some show traces of impact and wear, but others do not. Hammerstones were found on the earlier floor level and in overlying slag-bearing deposits. Pieces of worked antler were also found during excavation, with one perforated piece reminiscent of a bronze age mining pick from Cornwall (Timberlake, 2017:717) (**figure 5**). Given the proximity of major ore deposits on both sides of the modern Georgian-

Armenian border, not to mention the documented evidence for mining in Kvemo Kartli at least as early as 3000 BC (Stöllner and Gambashidze, 2011), it would not be surprising to find traces of mining implements at metallurgical sites. At the same time, hammerstones and worked antler could be used for a variety of different tools, and both antler pieces and hammerstones are also found in contexts without other clear metallurgical debris.

Samples of metallurgical debris were prepared for microscopic and chemical analysis to determine types of metal worked and the stages of production carried out at the site. Samples were prepared as polished blocks and examined using reflected light polarizing optical microscopy and scanning electron microscopy with an energy dispersive spectrometer for area and spot microanalysis to assist in phase identification. A JEOL JSM6460LV system fitted with both EDS and WDS spectrometers was used for analysis. To determine the chemical composition of molten fraction of the slag slags, EDS area analyses were carried out on a minimum of four different areas wherever possible, avoiding voids, corroded areas, and partially-reacted inclusions. As slags can be chemically and microstructurally heterogeneous, individual area analyses were averaged together. In some cases, particularly the lighter vesicular slags, the material was only partly vitrified, so it was not possible to analyze fully-molten areas. Samples sometimes displayed significant compositional heterogeneity even within the fully melted zones, as clearly reflected by the varying proportions of iron oxide, fayalite, and vitreous phases (see **figure 6A**).

A wavelength-dispersive spectrometer (WDS) was used to measure the composition of small particles and prills of metal trapped within the slags. Some prills had multiple discrete phases which were analyzed separately. Occasionally, (e.g. the arsenic-rich analyses in US191 prills) phase texturing was so fine that it was impossible to analyze each phase separately. Wherever possible, analyses were done on the largest prills or prill phases available, in order to minimize the possibility that the excitation volume extended outside the phase of interest. However, a few analyzed prills were quite small, and those analyses may be influenced by the composition of the surrounding material—either the slag, or the other phases within the metal particle. This potential issue was considered during analysis, but did not affect the overall interpretation. Analytical totals for the WDS analyses were all above 90%, with the majority between 94-100%. Of the two analyses with the lowest analytical totals (prills 15 and 19b), the former was on a very small prill (<10μm), making it subject to the issue discussed above, and the

latter was on a prill that showed some evidence of texture or possible oxidation. Two analyses (prills 8 and 9) had unusually high analytical totals, but since they match compositionally with an analysis of a similar prill from the same sample (prill 6) which yielded an analytical total very close to 100%, we report all three analyses. Encouragingly, some of the analyses with most unusual compositions (e.g. those with >30 wt.% As) had totals very close to 100%.

Analytical Results

The mineralogy and microstructure of the dense slags displayed all the hallmarks of iron smithing (See table S1 in supplementary information for individual sample descriptions; for hundreds of additional optical microscope and SEM images, see Erb-Satullo, et al., 2020b). They consisted of varying proportions of iron silicates (fayalite), iron oxide, and an interstitial glassy phase (**figure 6**). Iron oxides were predominantly wüstite (often with a characteristic dendritic morphology), but magnetite (identified by angular, equant crystals and slightly lower reflectance relative to wüstite) was also observed, indicating variable redox conditions. Aside from their characteristic macroscopic morphology, their identification as iron smithing slags is demonstrated by the presence of clusters of iron oxide that preserve the structure of flakes of hammerscale that have fallen onto the surface of the slag, but did not fully homogenize with the rest of the melt. These relict flakes of hammerscale are often found nearer the upper surface of the slag cake (**figure 6**). The small dribble of dense slag (SR216) from the same context as the two radiocarbon dates (SR218 and SR220) has a similar microstructure to the smithing hearth bottom slags, indicating that it formed through a similar process.

In terms of chemical composition, the dense slags are rich in iron (up to 79 wt.% FeO) with the silicon, aluminum, and calcium comprising the majority of the rest (**table 2**). Copper was not detected above the detection limit (estimated at 0.2 wt.%) in any of EDS area averages, except the slag adhering to the crucible rim (see below). Such bulk chemical compositions are roughly consistent with early iron smithing slags from other sites in the Near East (Erb-Satullo and Walton, 2017; Veldhuijzen and Rehren, 2007).

Metallic iron is a frequently occurring phase in both iron smelting and smithing slags. Unsurprisingly, particles of metallic iron were identified in many of the Mtsvane Gora slags (**figure 7**). Additionally, some samples contained iron corrosion products with morphologies

indicating that they were once metallic iron. For instance, a larger corroded metallic iron chunk in sample 33004-1 preserved a relict ferrite-pearlite microstructure, with an estimated 0.2% C, a carbon content putting in the range of low carbon iron (0-0.3% C) (**figure 7C**). EDS analysis of some metal particles revealed the presence of unusual elements, such as Cu, As, Ni, Sn, that were not detected in the bulk chemical composition of the slag as measured via area analyses.

In order to better characterize the composition of these particles, 27 analyses on 24 metallic particles in 9 slag samples were obtained via WDS microanalysis, which has a lower limit of detection than EDS analysis. These analyses revealed a variety of different compositions for metal particles trapped in the dense slags, and in the slag on the crucible rim, US217 (**table 3**). Some particles were nearly pure iron, with less than 0.30% Cu, As, Ni, Sn, and Co. Others metal particles contained significant amounts of one or more of these five elements. Arsenic content over 30 wt.% was measured in several prills in US191, while prills (or phases within prills) containing over 80 wt.% Cu were detected in samples US191, US194-2, and SR460-1. Notably, all these samples displayed the characteristic macroscopic, microscopic and mineralogical features of iron metallurgical slags. Sn (up to 10.14 wt.%), Ni (up to 8.22 wt.%) and Co (up to 0.53 wt%) were also detected. In some copper-rich phases, low levels of Sb (up to 0.72 wt.%) were also present. Cobalt and nickel are siderophile elements sometimes present in iron artifacts, but Cu, As, Sn, and Sb are atypical for iron metalworking debris. However, Cu, As, and Sb are common in polymetallic sulfide ores exploited in the Bronze Age Caucasus, and Sn is a common alloying element with some evidence for local exploitation by the end of the 2nd millennium BC (Erb-Satullo, et al., 2015). More unusual compositions were found in rounded speiss prills consisting of cupriferous iron arsenide in sample US191 (**figure 7D**), and in copper-base prills with 9-10% Sn and less than 8% Fe in sample US194-2. Sometimes, different species of prills were observed in the same sample: both US194-2 and US191 also contain metallic iron-base metallic prills with a lower Cu and As content, suggesting a high degree of heterogeneity in the melt. While the compositions of microscopic prills almost certainly do not match the bulk composition of the metallic product precisely, they do provide an indication of what metals were present in the furnace or hearth.

Microscopy of the slagged technical ceramic rim fragment (sample US217) revealed a small slagged area near the rim with abundant tiny prills of metallic copper, which contained 1.76% arsenic (**table 3**). The slag itself was mostly vitreous—a product of the melting technical

ceramic, but also contained several prills of iron- and copper-iron sulfides. Copper- and iron-sulfides are common in smelting slags, but considering the broader assemblage, it is more likely that the crucible was used for secondary casting or refining processes rather than smelting, and that these sulfides derive from sulfide inclusions in the raw copper metal.

Analysis of the slagged rock fragments and vesicular slags show microstructures indicating variable degrees of vitrification, from complete melting to partial and incipient vitrification, sometimes within the same sample (**figure 8**). These samples were mostly free of iron oxide and fayalite phases, except at the edges of some samples where they reacted with iron in the hearth. Occasional small metallic iron particles were observed, probably resulting from the in-situ reduction of detrital iron oxides in the hearth material. Iron sulfides were also occasionally observed within the melted or partly melted inclusions. However, their low frequency, small size, and clear association with partly reacted siliceous phases, suggest that they are also detrital heavy minerals deriving from the clays or other hearth materials.

Chemically, the vesicular slags are much lower in iron and richer in Si, Al, and Ca relative to the dense slags. This pattern suggests that the vitrified vesicular materials contained considerable input from clay and fuel ash, which may have acted as a fluxing agents that induced the vitrification. The potential contribution of fuel ash to these slags is indicated through comparison of three areas analyzed on the tuyère sample—the ceramic body, a zone of fully melted ceramic at the tip, and a small piece iron-rich slag adhering to the borehole. The melted tip is enriched in calcium relative to the more minimally-altered ceramic body, despite the fact that the melted tip contains only marginally more iron. The droplet of iron-rich slag adhering to the tuyère borehole is also enriched in calcium relative to the non-vitrified tuyère fabric. A similar pattern is seen when comparing fully melted with partially vitrified areas in sample SR141. SR141 consists of both partly vitrified low-iron materials and an iron-enriched areas that were fully molten, further confirming the metallurgical origin of the vesicular vitrified slags.

Microscopy and microanalysis showed that the crumbly yellow-orange material with brassy yellow inclusions consisted of iron sulfide (pyrite, FeS_2) inclusions within a matrix of jarosite ($KFe^{3+}{}_3(OH)_6(SO_4)_2$), with rarer inclusions of elemental sulfur (**figure 9**). This fragment likely derives from one of the nearby polymetallic sulfide deposits, where jarosite has been documented (e.g. Migineishvili, 2005:129) (**figure 1**). The oxidized zones of such deposits often contain oxide, carbonate and sulfate minerals.

Analysis of the magnetic fraction of later phase sediment from trench 1 (SR722b) revealed further microscopic traces of ironworking. Characteristic flakes of hammerscale diagnostic of iron smithing were identified, correlating with the partly reacted flakes trapped near the upper surfaces of some slag cakes (**figure 10**). Additional small particles of wüstite and fayalite-rich slag were also identified from these sediments. This microdebris reinforces the suggestion that ironworking activities took place close by, as any substantial erosional transport processes would destroy fragile hammerscale flakes or segregate it from the macrodebris.

Discussion

The overall microstructural and mineralogical homogeneity of the dense iron-rich slags, contrasts with the diversity seen in the compositions of metallic particles trapped within them. The presence of Cu, As, and Sn, even at low levels when considered in terms of bulk slag composition, points to a connection with copper-alloy metallurgy, while the presence of iron metal, abundant wüstite, and hammerscale points strongly towards their identification as iron smithing slags. These results have several possible interpretations. The most likely explanation is that the cross-contamination of iron smithing residues with copper and other chalcophile elements occurred because metalworkers were working iron and copper-alloys in the same hearths. In this scenario, Cu, As, and Sn from casting spillage or oxidized crusts fallen from metal objects annealing in the hearth, became incorporated along with hammerscale, iron slag droplets, and hearth material into the smithing hearth bottom. The redox conditions in the smithing hearth were strong enough to reduce these metals, which were then concentrated in the metallic phases. The presence of tin supports this interpretation. While recent research has suggested some tin ores in the Caucasus were exploited in the Bronze Age, it was mostly added to copper after the smelting stage (Erb-Satullo, et al., 2015). Thus, the co-occurrence of copper and tin suggests that the contamination happened after alloying. Some prill compositions suggest that metalworkers at Mtsvane Gora were creating alloys, not simply working alloys made elsewhere. The high-arsenic cupriferous speiss prills in Sample US-191 are best explained as a residue of alloying copper and arsenic though the mixing of copper metal and iron arsenide (speiss). Evidence for the production of speiss as an intermediary product for the manufacture of copper-arsenic alloys has been proposed elsewhere in the Near East (Rehren, et al., 2012;

Thornton, et al., 2009). The comparison of raw copper ingot fragments and finished objects from the western Caucasus (Abesadze and Bakhtadze, 2011 [1988]:346-365) also strongly suggests that, as with tin, arsenic was also added after the raw copper was smelted.

Another possible mechanism for the introduction of chalcophile elements must also be considered—the original ore used to smelt the iron. The adventitious discovery of iron smelting through experimentation with iron-rich gossans overlying copper deposits has been much hypothesized, but never conclusively demonstrated (Erb-Satullo, 2019:575-576; Merkel and Barrett, 2000). If iron gossans overlying polymetallic sulfide deposits were exploited for iron, one might expect the production residues to be contaminated with low levels of chalcophile elements. Iron metal in the bloom, and the slag attached to it, might be contaminated with such elements and could conceivably transfer them to smithing slags. In the case of the Mtsvane Gora slags, however, the presence of tin, the identification of speiss prills, and the fact that the slags relate to secondary alloying and working rather than primary smelting, is more easily explained by the "workshop contamination" hypothesis than a "gossan exploitation" hypothesis. More convincing evidence of the latter would be traces of elements diagnostic of polymetallic ores in unequivocal iron smelting remains.

At the same time, the fragment of pyrite and jarosite, the possible mining tools, and the proximity of major polymetallic sulfide deposits 20-30 km up the Debeda gorge, all suggest some kind of link between mining and prospection of polymetallic deposits and the metalworkers at Mtsvane Gora. While no evidence for smelting was identified on site, the results suggest that iron metalworking at Mtsvane Gora was connected, at both at the workshop scale and potentially the landscape scale, to the broader enterprise of copper-alloy metallurgy. The nature of these relationships remains unclear, but the evidence argues against a scenario of total separation bronze and iron economies.

These results have implications for the innovation of iron in the Caucasus and ultimately, the spread of this technology across Eurasia. Prior to this study, all co-occurrences of iron and copper-alloy metallurgical debris in the Near East before 500 BC were restricted to the Levant (Eliyahu-Behar, et al., 2012; Erb-Satullo and Walton, 2017; Roames, 2011). It was unclear whether the co-occurrence of copper and iron metallurgical activities was a phenomenon specific to that region. Indeed, the iron-dominated assemblages at Karagündüz, the distinction between iron and bronze metalworkers in Hittite texts (Cordani, 2016:172-173), and the lack of clear

evidence for iron smelting at copper smelting sites (Merkel and Barrett, 2000), could have been marshalled as evidence for greater separation in the production and circulation of the two metals. The results from Mtsvane Gora suggest that this was not the case. The close association between iron and copper-alloy metallurgy would suggest that the spread of iron may have been facilitated by its incorporation into existing practices of copper-alloy metalworkers. This model is further supported by finds of bimetallic artifacts and mimicry of bronze forms and manufacturing techniques in early iron (for examples from Iran and the Caucasus, see Abramishvili, 1957; Erb-Satullo, 2016:287-288; Maxwell-Hyslop and Hodges, 1966; Muscarella, 2004).

In discussing the relationship between early iron and contemporary copper-alloy metallurgy, it is worth making the distinction that while secondary iron and copper *working* debris have been found together, substantial evidence that iron and copper *smelting* were practiced together has yet to be uncovered. At present, it is difficult to say whether this pattern is genuine, or an artifact of archaeological research patterns that make secondary metal workshops within settlements more common discoveries. Recent work in western Georgia has uncovered numerous copper and iron smelting sites, sometimes within the same area, but so far, they date to different periods. The closest coincidence of iron and copper smelting is in the region of Samegrelo, where an early 1st millennium BC copper smelting region transformed into an iron smelting center in the mid-late 1st millennium BC (Erb-Satullo, et al., 2017; Erb-Satullo, et al., 2018; Erb-Satullo, et al., 2020a). Thus, the extent of integration between bronze and early iron economies remains unclear; the evidence is robust for integration among secondary working sites, but weaker in relation to primary mining and smelting sites.

Models of iron innovation must consider the competing pressures on the metallurgical industries of the early Iron Age. An extensive preexisting bronze industry with abundant local supplies may delay the acceptance of a new metal, while accumulated metallurgical skills may accelerate the process of adoption. Untangling these competing pressures requires a detailed understanding of the regional metallurgical landscape: the stages of production, the location of workshop sites, and the types of metals produced. In combination with recent and ongoing reassessments of metallurgical sites in the South Caucasus, the data from Mtsvane Gora will help to clarify this picture in the South Caucasus.

With respect to the impact that copper-alloy technologies had on early iron innovation, it is important to consider two related but distinct dimensions of possible interaction. One is how

462 the relative spatial and economic organization of bronze and iron metallurgical activities
463 conditioned the process of *adoption*—i.e. the spread of iron metallurgical technologies. In
464 investigating this aspect of the relationship, one might examine the co-location of bronze and
465 iron metallurgical activities (both smelting and smithing) or the relative social contexts in which
466 production and consumption occurred. The second important aspect to consider is how such
467 relationships between industries might explain iron *invention*—i.e. the initial discovery and
468 systematization of technologies involved in the reduction of iron ores to metal. Investigating this
469 relationship requires specific attention to iron and copper smelting. Were early iron smelters
470 exploiting gossans associated with copper deposits? Were copper smelting practices capable of
471 accidentally producing usable metallic iron? Was copper and iron smelting carried out in the
472 same places? In the Near East, while there has been some research on LBA-EIA copper smelting
473 sites (e.g. Ben-Yosef, et al., 2019; Erb-Satullo, et al., 2014; Knapp and Kassianidou, 2008),
474 robust assemblages of iron smelting debris are far rarer (see Veldhuijzen and Rehren, 2007).
475 Both aspects of the relationship between iron and bronze metallurgy have received considerable
476 attention, though this distinction has rarely been explicitly articulated.
477 The metallurgical remains at Mtsvane Gora relate most directly to this first aspect. The
478 evidence for the co-production of iron and copper-alloy artifacts in the same physical spaces
479 suggests close integration of bronze and iron metalworkers, at least in the working stages of
480 manufacture. This has implications for the mechanism of technological transfer and adoption,
481 implying that existing networks of bronze craftsmen were instrumental in propagating new iron
482 technologies. With respect to the influence of copper-alloy metallurgy on iron invention, the lack
483 of direct evidence for smelting at the site means that we cannot demonstrate that the same people
484 were smelting both metals, nor that iron was smelted from the gossans of copper deposits. At the
485 same time, the piece of mixed pyrite and jarosite is intriguing. Without overinterpreting this
486 piece, at the very least it suggests that metalworkers at Mtsvane Gora, or people they were in
487 contact with, were gathering pieces of iron-rich minerals from sulfide deposits relatively close to
488 the site. The overall significance is not yet clear, but it might indicate a degree of integration
489 between iron and copper-alloy economies in the mining and smelting stages of the chaîne
490 opératoire.
491
492 **Conclusion**

Survey, excavation, and laboratory analyses revealed that, during an early period of iron use, iron was being manufactured in the same workshops as a range of other copper alloys. Metallurgical activity was concentrated in the 8th-6th century BC, and site was abandoned after the mid-1st millennium BC. Microchemical analysis of metal particles trapped within the slags was instrumental in demonstrating the close association between ferrous and non-ferrous metallurgy at a pivotal moment of iron adoption in the region. Analyses suggest that the metallurgical activities at Mtsvane Gora were mostly restricted to secondary smithing, casting, and alloying, rather than smelting. However, the discovery of a fragment of mixed pyrite and jarosite hints at unspecified links between the metalworkers at the site and the exploitation of major polymetallic sulfide deposits in the Lesser Caucasus foothills to the south and west. While iron smithing remains at Mtsvane Gora probably post-date the earliest finds of iron artefacts in the region, they are at present the earliest radiocarbon-dated, analytically-verified iron metallurgical debris in the Caucasus. Moreover, the remains dates to a period when the use of iron was intensifying, making them important to understanding the economic factors influencing to iron adoption.

When viewed in regional perspective, the results from Mtsvane Gora permit some speculation about models of iron innovation, particularly in relation to its eastward spread. Prior to this study, evidence for the co-location of iron and copper-alloy metallurgy in the Near East before 500 BC was restricted to the Levant (Eliyahu-Behar, et al., 2012; Roames, 2011), and little if any iron metallurgical debris (as opposed to finished iron objects) dating to before 500 BC from the Caucasus, Iran, or Central Asia has been analyzed (for smithing in southeast Arabia, see Stepanov, et al., 2020). The co-location copper-alloy and iron metallurgical activities supports an iron adoption model involving the incorporation of iron into the metallurgical repertoire of copper-alloy metalworkers, rather than the emergence of a social and or economically distinct group of iron smiths. At the same time, despite much speculation about the possibility of producing usable iron in the process of copper metallurgy (Erb-Satullo, 2019:575-576), no clear case of copper and iron *smelting* (i.e. reduction from ore to metal) occurring at the same site has ever been identified. Many models of iron adoption contrast iron and bronze economies, emphasizing that bronze economies were dependent on long distance exchange networks, while iron economies were organized around locally-available resources (Mirau,

1997:110-111; Veldhuijzen, 2012:238). The increasing evidence for integration of bronze and ironworking activities adds a new layer of complication, suggesting that at iron and bronze metallurgy were not fully separate, self-contained industries.

Could iron metallurgy may have propagated along pre-existing networks of bronzeworkers during the early phases of expansion, and only later developed in areas with abundant iron ores, but little pre-existing copper smelting tradition? What was the impact of preexisting copper-alloy traditions? It is tempting to draw an analogy with some models of early agricultural innovation (Binford, 1968; Flannery, 1969:76), and propose that innovation spread through marginal zones of major bronze producing areas, where metallurgical expertise was high, but existing copper-base resources were insufficient to meet the demand for metal. Such models remain speculative at this stage, but it is increasingly clear that these discussions must consider complex and fine-grained geographies of natural resources and technical skill. Careful analysis of metallurgical sites like Mtsvane Gora is fundamental to reconstructing these crafting landscapes.

Methodologically, this research illustrates the value of microanalysis of metallic iron particles in iron slags. Except for the single slagged technical ceramic rim with barely-visible traces of green corrosion, there was little other macroscopic evidence for copper-alloy metallurgy at the site. Only through microanalysis of metallic particles in the slag did the full extent of this workflow integration become clear. Intriguingly, on the Iberian peninsula, Renzi et al. (2013) noted some unusual compositions of metallic particles, containing Cu, As, Ni, and Sb, in slags they interpret as iron metallurgical remains. These discoveries parallel those at Mtsvane Gora, and hint at a broader phenomenon. The co-occurrence of iron and copper metallurgy may be far more widespread than previously suggested, as microanalysis of iron-base particles in iron slags are rarely published. In the Caucasus, the lack of analyses of metallurgical debris has meant that information on where and when iron artifacts were made is often derived from largely unverified reports and brief references repeated in subsequent publications. Research on metallurgical debris at Mtsvane Gora illustrates how a metallurgically-attuned excavation strategy, combined with the comprehensive analysis of a wide range of metallurgical residues, can begin to resolve these issues.

Acknowledgements

This research was supported by grants from the Rust Family Foundation, the American School of Prehistoric Research, and the American Research Institute of the South Caucasus. The DEM of the site in figure 2 was collected with the support of a Spatial Archaeometry Research Collaborations (SPARC) Grant, the funding for which ultimately derived from the U.S. National Science Foundation (BCS-1519660). The DEMs in figure 1 are from GTOPO30 and ASTER (a product of METI and NASA). Post-excavation research and writing was facilitated by a British Institute at Ankara Study Grant to Nathaniel Erb-Satullo. We thank the Project ARKK team members for their assistance with excavations, John Marston for the identification of charcoal samples, and the two anonymous reviewers whose comments strengthened the paper.

Figure Captions

Figure 1. Map of the South Caucasus showing the location of Mtsvane Gora and other relevant Late Bronze and Early Iron Age sites.
1.5 column

Figure 2. Map of Mtsvane Gora showing surface distribution of slag and excavation orthophoto. Note that initial survey in 2014 was done with a handheld GPS, with a lower relative accuracy than the total station mapping done from 2015 onwards.
2 column

Figure 3. Plan of Trench 1 floor surface with position of radiocarbon dated charcoal samples (black triangles). The position of SR220 and SR218 are shown for reference, but they were stratigraphically above the other features shown in this plan, as were the metallurgical slags.
1.5 column

Figure 4. Metallurgical debris from Mtsvane Gora, including slags, technical ceramics, and other vitrified materials.
1.5 column

Figure 5. Stone tools and antler artifacts recovered during excavation.
1.5 column

Figure 6. Optical photomicrographs (PPL) of iron smithing slags from Mtsvane Gora. A. Stitched image showing mineralogical and microstructural changes across a vertical section beginning from the top of a slag cake. B. Partly-reacted flake of hammerscale trapped in a smithing slag. C. Wüstite and magnetite illustrating variable reducing conditions in the hearth.
2 column

Figure 7. Optical photomicrographs of metallic phases in metallurgical slags from Mtsvane Gora. A. and B. Iron-base metallic particles slags containing wüstite and fayalite. C. Corroded low-carbon iron (estimated ~0.2% C) with corroded ferrite (Fe) and pearlite (Prl). D. Polymetallic speiss prill containing iron, copper, and arsenic in a wüstite-rich slag. Prill labels correspond to those in table 3.
2 column

Figure 8. SEM backscatter images of vesicular, vitrified low-Fe slags, showing varying levels of vitrification.
2 column

Figure 9. SEM backscatter image of the fragment of mixed jarosite (Js), pyrite (Py), and elemental sulfur (S) with associated EDS spectra.
2 column

Figure 10. Optical photomicrographs (PPL) (A, B) and SEM backscatter image (C) of hammerscale magnetically recovered from excavated sediments in trench 1.
2 column

Table Captions

Table 1. Radiocarbon dates from Mtsvane Gora.

Table 2. Normalized EDS area analyses of slags. All values represent the average of several measurements. For select, highly heterogeneous samples, averaged area analyses are reported for different parts of the sample (e.g. in the case of the slagged crucible sample US217, for the ceramic and slag portions.)

Table 3. Normalized WDS analyses of metal prills trapped within metallurgical slags. Letter suffixes on the prill numbers (e.g. 2a and 2b) indicate different phases within the same prill. All analyses are on prills from dense iron-rich slags except prill 10, which was from a slagged technical ceramic. bdl – below detection limit, nm – element not measured.

Table S1 (Online Supplementary Information). List of analyzed samples with detailed mineralogical and microstructural information. For the metallic prills/particles, X indicates the presence of a few instances, while XX indicates that metal particles are common throughout the sample, and — indicates that they were not observed. The "Free Iron Oxide" column describes the main species of iron oxide that has crystallized from the melt, as a rough indicator of the redox conditions with the hearth/furnace. Note that other iron oxides not listed in this column (e.g. detrital minerals and corrosion products) may be present in the sample.

References

Abesadze, T., Bakhtadze, R., 2011 [1988]. Kolkhuri kult'uris met'alurgiis ist'oriisatvis (On the history of the metallurgy of the Colchis Culture) (in Georgian with Russian summary), Georgian National Museum, Tbilisi.

Abramishvili, R., 1957. Samtavris samarovanze aghmochenili gviani brinjaos khanisa da rk'inis parto atvisebis khanis dzeglebis datarighebisatvis (On the question of the dating of monuments of the Late Bronze Age and period of wise use of iron, found in the Samtavro cemetery), Sakartvelos Sakhelmts'ipo Muzeumis Moambe 19-A and 21-B, 115-140.

Badaljan, R.S., Edens, C., Gorny, R., Kohl, P.L., Stronach, D., Tonikjan, A.V., Hamayakjan, S., Mandrikjan, S., Zardarjan, M., 1993. Preliminary report on the 1992 excavations at Horom, Armenia, Iran 31, 1-24.

Belli, O., 1991. Ore deposits and minig in Eastern Anatolia in the Urartian period: Silver, copper, and iron, in: Merhav, R. (Ed.), Urartu: A Metalworking Center in the First Millennium B.C.E, The Israel Museum, Jerusalem, pp. 15-41.

Ben-Yosef, E., Liss, B., Yagel, O.A., Tirosh, O., Najjar, M., Levy, T.E., 2019. Ancient technology and punctuated change: Detecting the emergence of the Edomite Kingdom in the Southern Levant, Plos One 14, e0221967.

Binford, L.R., 1968. Post-Pleistocene Adaptation, in: Binford, S.R., Binford, L.R. (Eds.), New perspectives in archaeology, Aldine, Chicago.

Burney, C., 1996. 'The highland sheep are sweeter...', in: Bunnens, G. (Ed.), Cultural Interaction in the Ancient Near East: Papers read at a symposium held at the University of Melbourne, Department of Classics and Archaeology (29-30 September 1994), Peeters, Louvain, pp. 1-15.

Çevik, Ö., 2008. Periodisation criteria for Iron Age chronology in Eastern Anatolia and neighboring regions, Ancient Near Eastern Studies 45, 1-20.

Çifçi, A., 2017. The Socio-Economic Organisation of the Urartian Kingdom, Brill, Leiden.

Cordani, V., 2016. The development of the Hittite iron industry. A reappraisal of the written sources, Die Welt des Orients 46, 162-176.

Danti, M., 2013. Late Bronze and Early Iron Age in northwestern Iran, in: Potts, D.T. (Ed.), Oxford handbook of ancient Iran, Oxford University Press, Oxford.

Eliyahu-Behar, A., Yahalom-Mack, N., Shilstein, S., Zukerman, A., Shafer-Elliot, Maeir, A.M., Boaretto, E., Finkelstein, I., Weiner, S., 2012. Iron and bronze production in Iron Age IIA Philistia: New evidence from Tell es-Safi/Gath, Israel, Journal of Archaeological Science 39, 255-267.

Erb-Satullo, N., 2016. Metal production in the land of the Golden Fleece: Economic organization and technological change in the South Caucasus, 1500-500 BC, Unpublished PhD Dissertation, Department of Anthropology, Harvard University, Cambridge.

Erb-Satullo, N.L., Gilmour, B.J.J., Khakhutaishvili, N., 2014. Late Bronze Age and Early Iron Age copper smelting technologies in the South Caucasus: The view from ancient Colchis c. 1500-600 BC, Journal of Archaeological Science 49, 147-159.

Erb-Satullo, N.L., Gilmour, B.J.J., Khakhutaishvili, N., 2015. Crucible technologies in the Late Bronze-Early Iron Age South Caucasus: Copper processing, tin bronze production, and the possibility of local tin ores, Journal of Archaeological Science 61, 260-276.

Erb-Satullo, N.L., Gilmour, B.J.J., Khakhutaishvili, N., 2017. Copper production landscapes of the South Caucasus, Journal of Anthropological Archaeology 47, 109-126.

Erb-Satullo, N.L., Walton, J.T., 2017. Iron and copper production at Iron Age Ashkelon: Implications for the organization of Levantine metal production, Journal of Archaeological Science: Reports 15, 8-19.

Erb-Satullo, N.L., 2018. Patterns of settlement and metallurgy in Late Bronze-Early Iron Age Kvemo Kartli, southern Georgia, in: Anderson, W., Hopper, K., Robinson, A. (Eds.), Finding Common Ground in Diverse Environments: Landscape Archaeology in the South Caucasus, OREA, Austrian Academy of Sciences, Vienna, pp. 37-52.

Erb-Satullo, N.L., Gilmour, B.J.J., Khakhutaishvili, N., 2018. The ebb and flow of copper and iron smelting in the South Caucasus, Radiocarbon 60, 159-180.

Erb-Satullo, N.L., 2019. The innovation and adoption of iron in the ancient Near East, Journal of Archaeological Research 27, 557-607.

Erb-Satullo, N.L., Jachvliani, D., Kalayci, T., Puturidze, M., Simon, K., 2019. Investigating the spatial organisation of Bronze and Iron Age fortress complexes in the South Caucasus, Antiquity 93, 412-431.

Erb-Satullo, N.L., Gilmour, B.J.J., Khakhutaishvili, N., 2020a. The metal behind the myths: Iron smelting in the southeastern Black Sea region, Antiquity 94, 401-419.

Erb-Satullo, N.L., Jachvliani, D., Kakhiani, K., Newman, R., 2020b. Optical and Scanning Electron Microscope Images of Metallurgical Debris from Mtsvane Gora, https://doi.org/10.7910/DVN/R1UYEL, Harvard Dataverse, Version 1.0.

Flannery, K.V., 1969. Origins and ecological effects of early domestication in Iran and the Near East, in: Ucko, P.J., Dimbleby, G.W. (Eds.), The domestication and exploitation of plants and animals, Duckworth, London, pp. 73-100.

Gale, N.H., Bachmann, H.G., Rothenberg, B., Stos-Gale, Z.A., Tylecote, R.F., 1990. The adventitious production of iron in the smelting of copper, in: Rothenberg, B. (Ed.), The Ancient Metallurgy of Copper, Institute for Archaeo-Metallurgical Studies, Institute of Archaeology, University College London, London, pp. 182-191.

Gottlieb, Y., 2010. The advent of the age of iron in the land of Israel: A review and reassessment, Tel Aviv 37, 89-110.

Gzelishvili, I.A., 1964. Zhelezoplavil'noe Proizvodstvo v Drevney Gruzii (Iron Smelting Production in Ancient Georgia), Metsniereba, Tbilisi.

741 Japaridze, O., 1999. From the Middle Bronze to the Early Iron Age in Georgia, in: Soltes, O.Z.
742 (Ed.), National Treasures of Georgia, Philip Wilson Ltd., London, pp. 62-65.
743
744 Johnson, D., Tylsesley, J., Lowe, T., Withers, P.J., Grady, M.M., 2013. Analysis of a prehistoric
745 Egyptian iron bead with implications for the use and perception of meteorite iron in ancient
746 Egypt, Meteoritics and Planetary Science 48, 997-1006.
747
748 Kaufman, B., Docter, R., Fischer, C., Chelbi, F., Maraoui Telmini, B., 2016. Ferrous metallurgy
749 from the Bir Massouda metallurgical precinct at Phoenician and Punic Carthage and the
750 beginning of the North African Iron Age, Journal of Archaeological Science 71, 33-50.
751
752 Khakhutaishvili, D.A., 1987. Proizvodstvo Zheleza v Drevney Kolkhide (The Production of Iron
753 in Ancient Colchis), Metsniereba, Tbilisi.
754
755 Khanzadian, E., 1995. Metsamor 2: La Necropole, Volume 1, Les Tombes du Bronze Moyen et
756 Recent, Academie Nationale des Science d'Armenie: Institute d'Archeologie et d'Ethnographie,
757 Neuchâtel.
758
759 Khatchadourian, L., 2018. Pottery typology and craft learning in the Near Eastern highlands,
760 Iranica Antiqua 53, 179-265.
761
762 Knapp, A.B., Kassianidou, V., 2008. The archaeology of Late Bronze Age copper production:
763 Politiko Phorades on Cyprus, in: Yalçin, Ü. (Ed.), Anatolian Metal IV, Bochum Vereinigung der
764 Freunde von Kunst und Kultur im Bergbau, Bochum, Germany, pp. 135-147.
765
766 Köruoğlu, K., Konyar, E., 2008. Comments on the Early/Middle Iron Age chronology of the
767 Lake Van Basin, Ancient Near Eastern Studies 45, 123-146.
768
769 Lam, W., 2014. Everything old is new again? Rethinking the transition to cast iron production in
770 the Central Plains of China, Journal of Anthropological Research 70, 511-542.
771
772 Maddin, R., 1975. Early iron metallurgy in the Near East, Transactions of the Iron and Steel
773 Institute of Japan 15, 59-68.
774
775 Martirosyan, A.A., 1974. Argishtikhinili, Akademii Nauk Armyanskoy SSR, Erevan.
776
777 Maxwell-Hyslop, K.R., Hodges, H.W.M., 1966. Three iron swords from Luristan, Iraq 28, 164-
778 176.
779
780 McClellan, J.A., 1975. Iron Objects from Gordion: A Typological and Functional Analysis, PhD
781 dissertation, Department of Classical Archaeology, University of Pennsylvania, Philadelphia.
782
783 McConchie, M., 2004. Archaeology at the North-East Anatolian Frontier, V: Iron Technology
784 and Iron Making Communities of the First Millennium BC, Peeters, Louvain, Belgium.
785

786 Merkel, J.F., Barrett, K., 2000. 'The adventitious production of iron in the smelting of copper'
787 revisited: Metallographic evidence against a tempting model., Historical Metallurgy 34, 59-66.
788
789 Migineishvili, R., 2005. Hybrid nature of the Madneuli Cu-Au deposit, Georgia, in: Cook, N.J.,
790 Bonev, I.K. (Eds.), International Geological Correlation Programme, Project 486. Proceedings of
791 the 2005 Field Workshop, Kiten, Bulgaria 14-19 September 2005, Bulgarian Academy of
792 Sciences, Sofia, pp. 128-132.
793
794 Mirau, N.A., 1997. Social context of early ironworking in the Levant, in: Aufrecht, W.A., Mirau,
795 N.A., Gauley, S.W. (Eds.), Urbanism in Antiquity: From Mespotamia to Crete, Sheffield
796 Academic Press, Sheffield, UK, pp. 99-115.
797
798 Muscarella, O.W., 2004. The Hasanlu lion pins again, in: Sagona, A. (Ed.), A view from the
799 highlands: archaeological studies in honor of Charles Burney, Peeters, Louvain, pp. 693-710.
800
801 Nieling, J., 2009. Die Einführung der Eisentechnologie in Südkaukasien und Ostanatolien
802 wahrend der Spätbronze- und Früheisenzeit, Aarhus University Press, Aarhus.
803
804 Papuashvili, R., 2011. K voprosu ob absolyutnoy khronologii mogil'nikov kolkhidy epokhi
805 pozdney bronzy-rannego zheleza (On the question of the absolute chronology of the cemeteries
806 of Colchis in the Late Bronze - Early Iron Age), in: Albegova, Z.K., Bagaev, M.K., Korenevskiy,
807 S.N. (Eds.), Voprosy Drevney i Srednevekovoy Arkheologii Kavkaza (Questions of Ancient and
808 Medieval Archaeology of the Caucasus), Uchrezhdeniye Rossiyskoy Akademii Nauk Institut
809 Arkheologii, Grozny, Russia, pp. 82-94.
810
811 Rehren, T., Boscher, L., Pernicka, E., 2012. Large scale smelting of speiss and arsenical copper
812 at Early Bronze Age Arisman, Iran, Journal of Archaeological Science 39, 1717-1727.
813
814 Rehren, T., Belgya, T., Jambon, A., Káli, G., Kasztovszky, Z., Kis, Z., Kovács, I., Maróti, B.,
815 Martinón-Torres, M., Miniaci, G., Pigott, V.C., Radivojević, M., Rosta, L., Szentmiklósi, L.,
816 Szőkefalvi-Nagy, Z., 2013. 5,000 years old Egyptian iron beads made from hammered meteoritic
817 iron, Journal of Archaeological Science 40, 4785-4792.
818
819 Renzi, M., Rovira, S., Rovira-Hortalà, M.C., Montero Ruiz, I., 2013. Questioning research on
820 early iron in the Mediterranean, in: Humphris, J., Rehren, T. (Eds.), The World of Iron,
821 Archetype Publications, London, pp. 178-187.
822
823 Roames, J., 2011. The Early Iron Age metal workshop at Tell Tayinat, Turkey, in: Vandiver, P.,
824 Li, W., Ruvalcaba Sil, J.L., Reedy, C.L., Frame, L.D. (Eds.), Materials Issues in Art and
825 Archaeology IX, Cambridge University Press, Cambridge, pp. 149-155.
826
827 Snodgrass, A.M., 1980. Iron and Early Metallurgy in the Mediterranean, in: Wertime, T.A.,
828 Muhly, J.D. (Eds.), The Coming of the Age of Iron, Yale University Press, New Haven, pp. 335-
829 374.
830

831 Stepanov, I.S., Weeks, L., Franke, K.A., Overlaet, B., Alard, O., Cable, C.M., Al Aali, Y.Y.,
832 Boraik, M., Zein, H., Grave, P., 2020. The provenance of early Iron Age ferrous remains from
833 southeastern Arabia, Journal of Archaeological Science 120.
834
835 Stöllner, T., Gambashidze, I., 2011. Gold in Georgia II: The oldest gold mine in the world, in:
836 Yalçin, Ü. (Ed.), Anatolian Metal V, Deutsches Bergbau-Museum, Bochum, Germany, pp. 187-
837 199.
838
839 Stöllner, T., Gambashidze, I., 2014. The gold mine of Sakdrisi and the earliest mining and
840 metallurgy in the Transcaucasus and the Kura-valley system, in: Narimanishvili, G. (Ed.),
841 Problems of Early Metal Age Archaeology of Caucasus and Anatolia Georgian National
842 Museum, Tbilisi, pp. 102-124.
843
844 Thornton, C.P., Rehren, T., Pigott, V.C., 2009. The production of speiss (iron arsenide) during
845 the Early Bronze Age in Iran, Journal of Archaeological Science 36, 308-316.
846
847 Timberlake, S., 2017. New ideas on the exploitation of copper, tin, gold, and lead ores in Bronze
848 Age Britain: The mining, smelting, and movement of metal, Materials and Manufacturing
849 Processes 32, 709-727.
850
851 Veldhuijzen, H.A., Rehren, T., 2007. Slags and the city: Early iron production at Tell Hammeh,
852 Jordan and Tel Beth-Shemesh, Israel, in: La Niece, S., Hook, D., Craddock, P. (Eds.), Metals and
853 Mines: Studies in Archaeometallurgy, Archetype Publications, London, pp. 189-201.
854
855 Veldhuijzen, H.A., 2012. Just a few rusty bits: The innovation of iron in the Eastern
856 Mediterranean in the 2nd and 1st millennia BC, in: Kassianidou, V., Papasavvas, G. (Eds.),
857 Eastern Mediterranean Metallurgy and Metalwork in the Second Millennium BC, Oxbow Books,
858 Oxford, pp. 237-250.
859
860 Yahalom-Mack, N., Eliyahu-Behar, A., 2015. The transition from bronze to iron in Canaan:
861 Chronology, technology and context, Radiocarbon 57, 285-305.

Table 1. Radiocarbon dates from Mtsvane Gora.

Lab #	Field #	Context	Material	Uncalibrated Date (RC yrs BP)	Calibrated data (Calibrated 2σ Date Ranges)
AA107057	SR218	Trench 1, deposits containing metallurgical debris, above earlier floor level	Wood charcoal (immature wood, short-lived, possible *Carpinus sp.*)	2465±22	763-479 BC (94.2%); 444-432 BC (1.2%)
AA107060	SR220	Trench 1, deposits containing metallurgical debris, above earlier floor level	Wood charcoal (immature wood, short-lived, possible *Carpinus sp.*)	2474±27	770-482 BC (94.7%); 442-434 BC (0.7%)
AA110425	SR596	Trench 1, sample on clay floor	Wood charcoal (conifer, possible *Juniperus sp.*)	3026±25	1391-1337 BC (21.8%); 1322-1207 BC (73.6%)
AA110426	SR1033	Trench 1, sample on clay floor near base of fortification wall	Wood charoal (short-lived branch, *Quercus sp.*)	3017±25	1387-1340 BC (14.5%); 1311-1192 BC (79.1%); 1172-1169 BC (0.3%); 1143-1132 BC (1.6%)
AA110922	SR517	Trench 4, near set of whole vessels	Wood charcoal (possible *Fraxinus sp.*)	3151±33	1501-1381 BC (86.2%); 1341-1308 BC (9.2%)

Table 2

Table 2. Normalized EDS area analyses of slags. All values represent the average of several measurements. For select, highly heterogeneous samples, averaged area ar

Sample #	Sample Descr.	Descr. of Area Analyzed	Na_2O	MgO	Al_2O_3	SiO_2	P_2O_5	SO_2	K_2O	CaO	TiO_2	MnO	FeO
17SLG-1	Plano-convex dense slag cake	Fully melted slag area	1.6	1.2	7.6	25.6	0.4	bdl	1.4	5.2	0.2	bdl	56.8
17SLG-2	Dense slag fragment	Fully melted slag area	1.3	1.8	9.0	29.1	0.9	bdl	2.5	8.2	0.3	bdl	47.0
17SLG-3	Dense slag fragment	Fully melted slag area	1.6	1.2	6.7	21.7	0.3	bdl	1.1	3.9	0.2	bdl	63.4
17SLG-4	Concavo-convex dense slag cake fragment	Fully melted slag area	1.0	1.2	6.6	18.5	1.2	bdl	1.0	5.4	0.2	0.2	64.7
33004-1	Dense slag cake fragment	Fully melted slag area	0.7	0.7	5.4	15.5	bdl	0.2	1.2	1.8	0.2	bdl	74.3
33006-2	Dense slag cake fragment	Fully melted slag area	2.0	1.8	9.2	34.3	0.8	bdl	2.4	8.8	0.4	bdl	40.3
33007-1	Dense slag cake fragment	Fully melted slag area	1.2	1.2	7.4	23.7	0.5	bdl	1.5	4.0	0.2	bdl	60.3
33007-2	Small dense slag fragment	Fully melted slag area	0.9	0.9	6.0	27.4	0.3	bdl	1.6	4.2	0.2	0.4	58.2
SR100	Small dense slag fragment	Fully melted slag area	1.5	1.0	5.8	18.5	0.4	0.2	1.0	4.8	0.2	bdl	66.6
SR141	Black vitreous slag piece	Fully melted slag area	1.3	3.2	8.3	39.4	1.2	bdl	2.9	11.9	0.5	bdl	31.4
SR141	Black vitreous slag piece	Partly vitrified area	0.8	0.5	9.4	81.8	bdl	bdl	2.9	3.0	0.3	bdl	1.3
SR207	Small piece of vesicular slag	Fully melted slag area	1.1	4.1	10.3	48.0	2.6	0.3	8.5	13.7	0.4	0.2	10.9
SR209	Black vitreous slag fragment	Fully melted slag area	1.2	1.8	8.6	35.5	0.8	0.4	2.5	9.4	0.5	bdl	39.3
SR216	Small dribble/splash of dense slag.	Fully melted slag area	0.5	0.6	3.6	17.8	0.3	0.2	1.3	2.6	0.2	bdl	73.0
SR245	Vesicular slag fragment	Partly vitrified area	1.5	2.9	16.6	66.5	0.2	0.2	2.9	2.3	1.2	bdl	5.8
SR255	Vesicular slag fragment	Fully melted slag area	1.5	3.7	15.5	52.7	0.2	bdl	2.1	17.7	0.9	bdl	5.7
SR255	Vesicular slag fragment	Partly vitrified area	1.4	3.5	16.3	54.9	0.4	0.2	2.8	12.2	1.1	bdl	7.3
SR259	Fused globules of black vitreous slag	Partly vitrified area	5.4	0.3	13.3	71.1	0.2	0.2	2.9	3.7	0.5	bdl	2.5
SR340	Vesicular slag fragment	Fully melted slag area	1.8	3.5	13.1	54.1	2.0	0.5	4.6	15.2	0.6	bdl	4.5
SR370	Plano-convex dense slag cake	Fully melted slag area	1.6	1.0	5.3	21.2	0.7	bdl	1.2	5.0	0.2	bdl	64.0
SR403	Small piece of vesicular slag	Partly-mostly vitrified area	1.7	3.3	14.5	60.2	0.9	bdl	4.7	9.3	0.7	0.2	4.6
SR410	Small piece of vesicular slag	Partly-mostly vitrified area	3.5	2.4	11.2	65.9	1.5	bdl	3.6	8.6	0.5	bdl	2.9
SR414	Small piece of vesicular slag	Partly vitrified area	1.6	3.4	16.2	64.5	0.3	bdl	2.7	3.2	1.0	0.2	6.8
SR460-1	Dense slag fragment	Fully melted slag area	1.5	1.6	6.6	30.3	1.0	0.2	1.6	8.8	0.2	bdl	48.2
SR460-2	Dense slag fragment	Fully melted slag area	4.3	2.6	16.0	61.5	0.3	bdl	3.0	6.8	0.5	bdl	5.0
SR478	Dense slag fragment	Fully melted slag area	0.7	0.6	5.0	12.1	0.2	0.2	1.1	2.1	bdl	bdl	78.0
SR700	Small piece of vesicular slag	Fully melted slag area	1.7	3.4	17.6	60.9	0.3	bdl	2.9	5.7	1.2	bdl	6.3
SR701	Small piece of vesicular slag	Partly vitrified area	1.4	3.2	17.0	65.6	0.2	bdl	2.9	1.9	1.1	0.2	6.5

SR71	Slag cake fragment (may join to slag cake SR 371)	Fully melted slag area	1.5	3.6	10.8	54.2	1.3	bdl	3.6	15.4	0.6	bdl	8.9
SR720	Small piece of vesicular slag	Partly-mostly vitrified area	1.5	3.4	12.2	60.4	1.3	bdl	5.5	10.8	0.6	bdl	4.1
SR721	Small piece of vesicular slag	Partly-mostly vitrified area	1.3	3.2	10.1	62.7	2.2	bdl	4.6	11.7	0.5	bdl	3.8
SR722a	Vesicular slag fragment from sediment sample	Partly vitrified area	2.7	2.6	16.7	62.6	0.2	bdl	4.5	4.6	0.7	bdl	5.4
SR722b	Small fragment of dense, iron-rich slag within magnetic fraction of sediment sample	Fully melted slag area	0.3	0.7	2.7	16.7	0.6	bdl	1.4	5.3	bdl	bdl	72.2
SR731	Small piece of vesicular slag	Partly vitrified area	2.0	2.5	12.0	63.0	2.2	bdl	4.1	9.8	0.5	bdl	4.0
SR788	Vesicular slag piece	Mostly vitrified area	1.6	4.6	12.5	55.9	0.9	0.2	3.0	15.1	0.6	0.2	5.3
SR955	Dense slag fragment	Fully melted slag area	0.6	0.8	3.9	19.6	0.5	0.2	1.1	5.6	0.0	0.5	67.2
Tuy1	Tuyère tip fragment	Ceramic	2.3	2.8	16.2	63.5	0.3	bdl	2.8	4.8	0.9	0.2	6.0
Tuy1	Tuyère tip fragment	Slagged area at tip of borehole	1.9	2.4	8.8	28.9	1.8	bdl	4.0	12.2	0.4	bdl	39.8
Tuy1	Tuyère tip fragment	Slagged area at tuyere tip	1.7	3.4	12.1	50.9	1.7	0.2	5.3	16.8	0.7	bdl	7.4
US191	Dense slag fragment	Fully melted slag area	1.1	1.4	6.8	25.3	0.7	bdl	2.3	6.0	0.2	bdl	56.1
US192	Dense slag fragment	Fully melted slag area	2.8	1.3	9.9	29.6	0.4	bdl	1.7	5.6	0.4	bdl	48.5
US193	Dense slag cake fragment	Fully melted slag area	0.5	0.7	2.9	12.4	0.5	bdl	1.0	3.1	bdl	bdl	79.0
US194-1	Dense slag cake fragment	Fully melted slag area	0.9	1.1	5.0	16.5	0.2	bdl	0.8	3.9	0.2	0.4	70.9
US194-2	Dense slag cake fragment	Fully melted slag area	1.4	0.9	4.4	18.1	0.5	bdl	1.3	5.5	bdl	bdl	67.8
US195	Dense slag fragment	Fully melted slag area	1.1	1.2	5.5	19.7	0.5	bdl	1.6	4.4	0.2	bdl	65.9
US196	Dense slag fragment	Fully melted slag area	0.9	1.0	7.8	24.5	0.4	bdl	2.3	4.9	0.2	bdl	58.1
US197	Black vitreous slag fragment	Fully melted slag area	1.2	5.1	16.3	52.3	0.4	bdl	1.4	12.2	1.1	0.4	9.6
US217	Slagged technical ceramic rim fragment	Ceramic fabric	3.5	3.2	16.5	62.3	0.3	bdl	2.4	4.2	0.9	0.2	6.3
US217	Slagged technical ceramic rim fragment	Fully melted slag area	4.0	2.6	14.8	50.9	0.4	0.2	2.6	11.9	0.5	bdl	5.3
US220	Slagged piece of rock	Fully melted area	1.9	3.6	11.2	54.4	2.2	0.5	5.3	16.8	0.6	0.2	3.4

ıalyses are reported for differe

NiO	CuO	As_2O_3	PbO
bdl	bdl	bdl	bdl
bdl	bdl	bdl	bdl
bdl	bdl	bdl	bdl
bdl	bdl	bdl	bdl
bdl	bdl	bdl	bdl
bdl	bdl	bdl	bdl
bdl	bdl	bdl	bdl
bdl	bdl	bdl	bdl
bdl	bdl	bdl	bdl
bdl	bdl	bdl	bdl
bdl	bdl	bdl	bdl
bdl	bdl	bdl	bdl
bdl	bdl	bdl	bdl
bdl	bdl	bdl	bdl
bdl	bdl	bdl	bdl
bdl	bdl	bdl	bdl
bdl	bdl	bdl	bdl
bdl	bdl	bdl	bdl
bdl	bdl	bdl	bdl
bdl	bdl	bdl	bdl
bdl	bdl	bdl	bdl
bdl	bdl	bdl	bdl
bdl	bdl	bdl	bdl
bdl	bdl	bdl	bdl
bdl	bdl	bdl	bdl
bdl	bdl	bdl	bdl
bdl	bdl	bdl	bdl
bdl	bdl	bdl	bdl

bdl	bdl	bdl	bdl
bdl	bdl	bdl	bdl
bdl	bdl	bdl	bdl
bdl	bdl	bdl	bdl
bdl	bdl	bdl	bdl
bdl	bdl	bdl	bdl
bdl	bdl	bdl	bdl
bdl	bdl	bdl	bdl
bdl	bdl	bdl	bdl
bdl	bdl	bdl	bdl
bdl	bdl	bdl	bdl
bdl	bdl	bdl	bdl
bdl	bdl	bdl	bdl
bdl	bdl	bdl	bdl
bdl	bdl	bdl	bdl
bdl	bdl	bdl	bdl
bdl	bdl	bdl	bdl
bdl	bdl	bdl	bdl
bdl	6.6	bdl	bdl
bdl	bdl	bdl	bdl

Table 3. Normalized WDS analyses of metal prills trapped within metallurgical slags. Letter suffixes on the prill numbers (e.g. 2a and 2b) indicate different phases within the same prill. All analyses are on prills from dense iron-rich slags except prill 10, which was from a slagged technical ceramic. bdl – below detection limit, nm – element not measured.

Prill #	Sample #	As	Cu	Ni	Co	Fe	Mn	Sb	Sn	Ag	Pb	S	P
1	US191	2.18	2.99	0.33	0.17	94.19	bdl	nm	bdl	bdl	0.13	nm	bdl
2a	US191	33.04	22.24	1.1	0.2	43.27	bdl	bdl	bdl	bdl	bdl	0.16	bdl
2b	US191	32.03	14.68	1.07	0.18	51.86	bdl	bdl	bdl	bdl	bdl	0.18	bdl
3a	US191	7.59	84.14	0.15	bdl	7.63	bdl	0.47	bdl	bdl	bdl	0.02	bdl
3b	US191	37.74	13.18	0.76	0.22	47.94	bdl	bdl	bdl	bdl	bdl	0.16	bdl
4	US193	0.12	bdl	0.04	0.12	99.71	bdl	nm	bdl	bdl	bdl	nm	bdl
5	US193	0.33	bdl	0.08	0.15	99.44	bdl	nm	bdl	bdl	bdl	nm	bdl
6	US194-2	1.43	81.08	0.67	0.06	7.63	bdl	bdl	9.12	bdl	bdl	0.02	bdl
7	US194-2	0.15	1.88	0.11	0.31	97.39	bdl	nm	0.11	0.04	bdl	nm	bdl
8	US194-2	0.64	82.17	1.02	0.06	5.98	bdl	nm	10.14	bdl	bdl	nm	bdl
9	US194-2	1.53	84.12	1.24	0.03	3.59	bdl	bdl	9.37	bdl	bdl	0.13	bdl
10	US217	1.76	97.46	bdl	bdl	0.65	bdl	nm	0.06	0.06	bdl	nm	bdl
11	33007-1	0.85	0.42	8.22	0.44	90.08	bdl	nm	bdl	bdl	bdl	nm	bdl
12	33007-1	0.21	2.87	1.1	0.53	95.3	bdl	nm	bdl	bdl	bdl	nm	bdl
13	33007-2	0.09	0.05	bdl	0.12	99.73	bdl	nm	bdl	bdl	bdl	nm	bdl
14	33007-2	0.13	0.08	0.05	0.29	99.45	bdl	nm	bdl	bdl	bdl	nm	bdl
15	SR216	0.35	0.08	0.13	0.21	99.23	bdl	nm	bdl	bdl	bdl	nm	bdl
16	SR216	0.2	0.22	0.04	0.18	99.33	0.03	bdl	bdl	bdl	bdl	bdl	bdl
17	SR460-1	0.53	1.19	1.02	0.25	97.01	bdl	nm	bdl	bdl	bdl	nm	bdl
18	SR460-1	2.1	2.49	1.75	0.27	93.32	bdl	0.04	bdl	bdl	bdl	0.04	bdl
19a	SR460-1	3.09	85.96	1.97	bdl	6.48	bdl	0.72	1.72	bdl	bdl	0.06	bdl
19b	SR460-1	9.11	2.75	5.47	0.28	82.09	bdl	bdl	0.04	bdl	bdl	0.25	bdl
20	SR478	0.12	0.11	bdl	0.19	99.57	bdl	nm	bdl	bdl	bdl	nm	bdl
21	SR478	0.27	0.09	0.18	0.27	99.19	bdl	nm	bdl	bdl	bdl	nm	bdl
22	SR955	0.12	0.04	bdl	0.23	99.59	bdl	bdl	bdl	bdl	bdl	0.02	bdl
23	SR955	0.17	bdl	bdl	0.22	99.59	bdl	bdl	bdl	bdl	bdl	0.02	bdl
24	SR955	0.15	bdl	bdl	0.22	99.53	bdl	bdl	bdl	bdl	0.08	0.02	bdl

Color Code	0.3-1	1.0-5.0	>5.0

Figure 1

Click here to access/download;Figure;Fig1_OverviewMap_labelled.tif

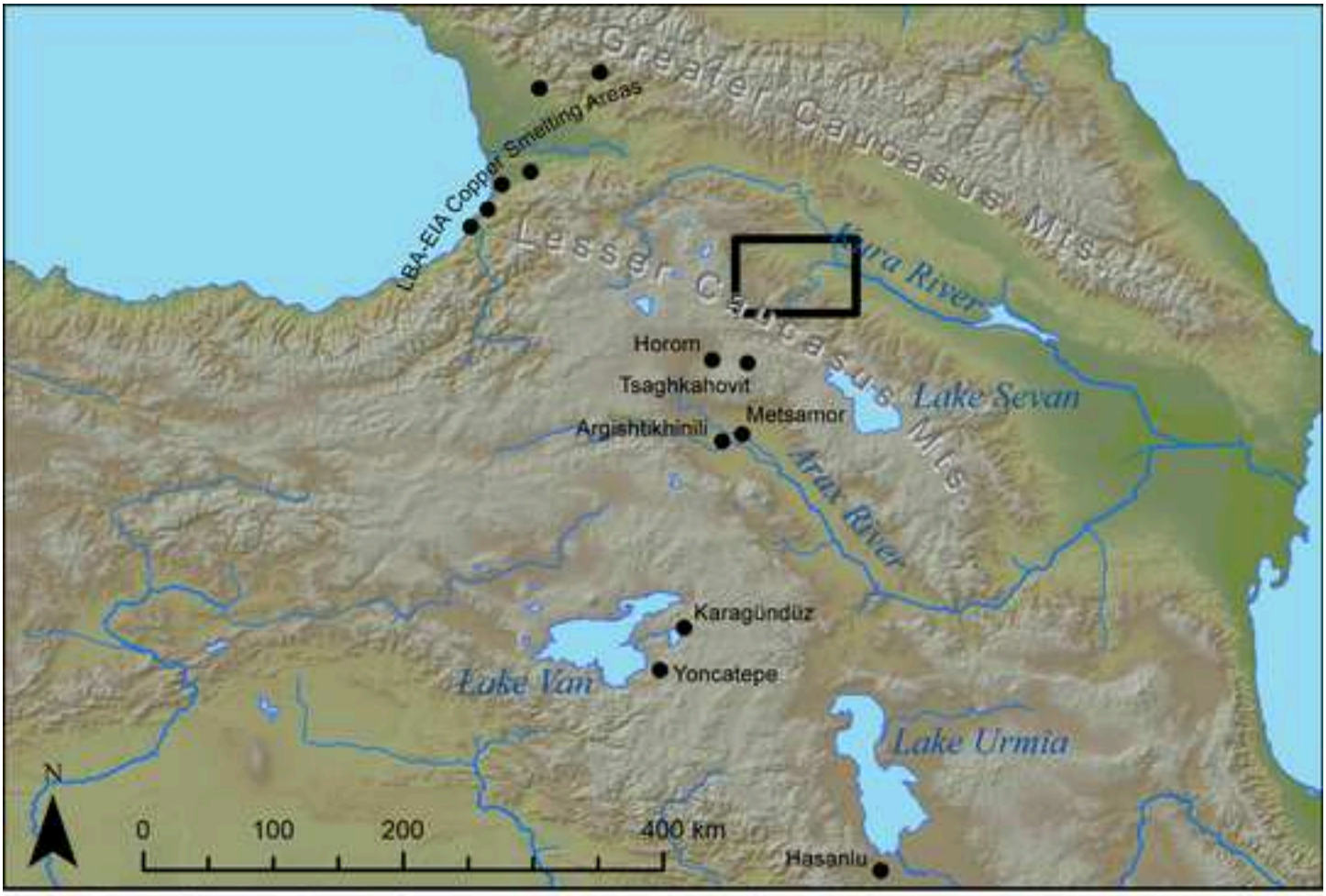

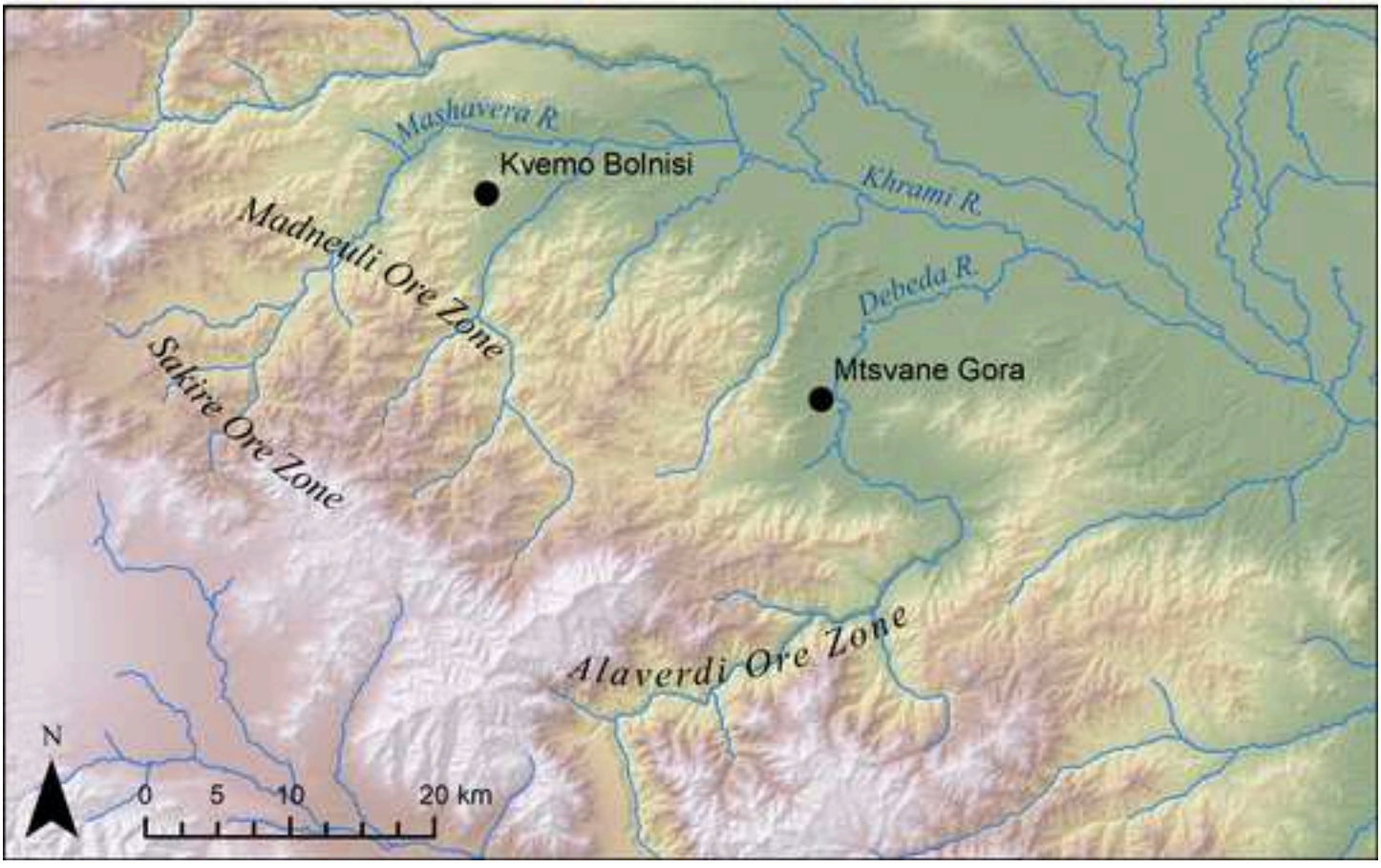

Figure 2

Click here to access/download;Figure;Fig2_SiteMap.jpg

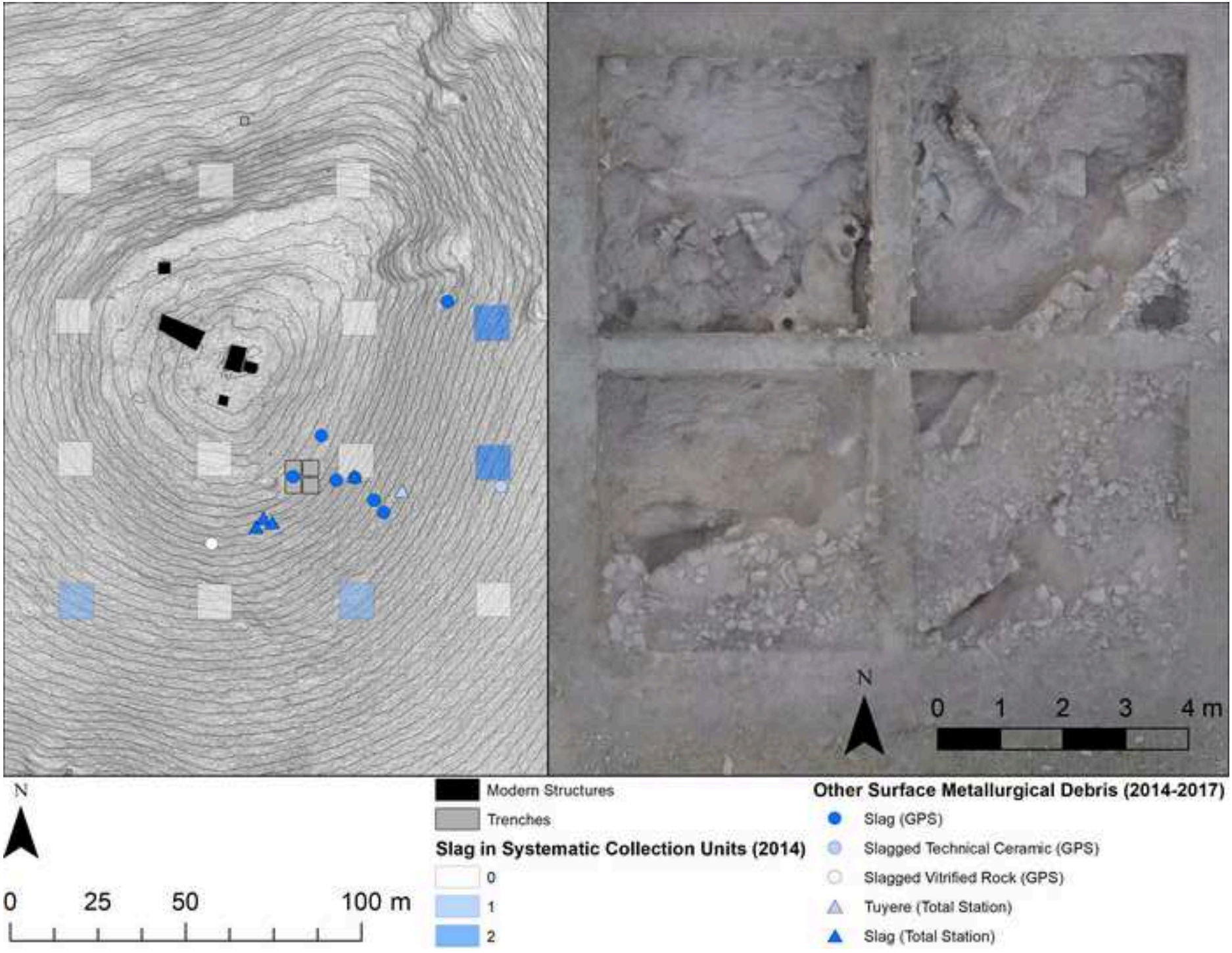

Figure 3

Click here to access/download;Figure;Fig3_Trench1Plan_labelled.tif

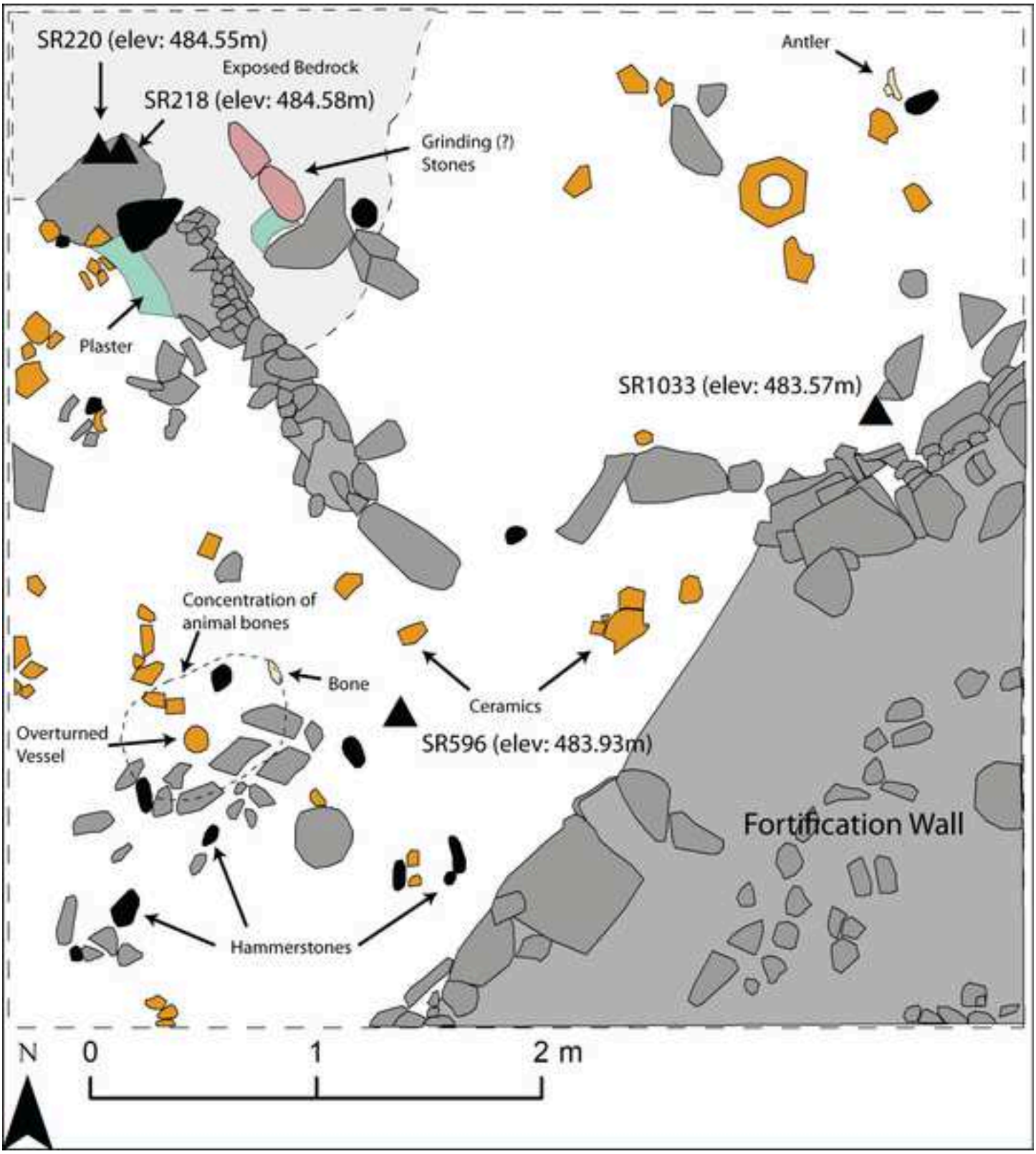

Figure 4

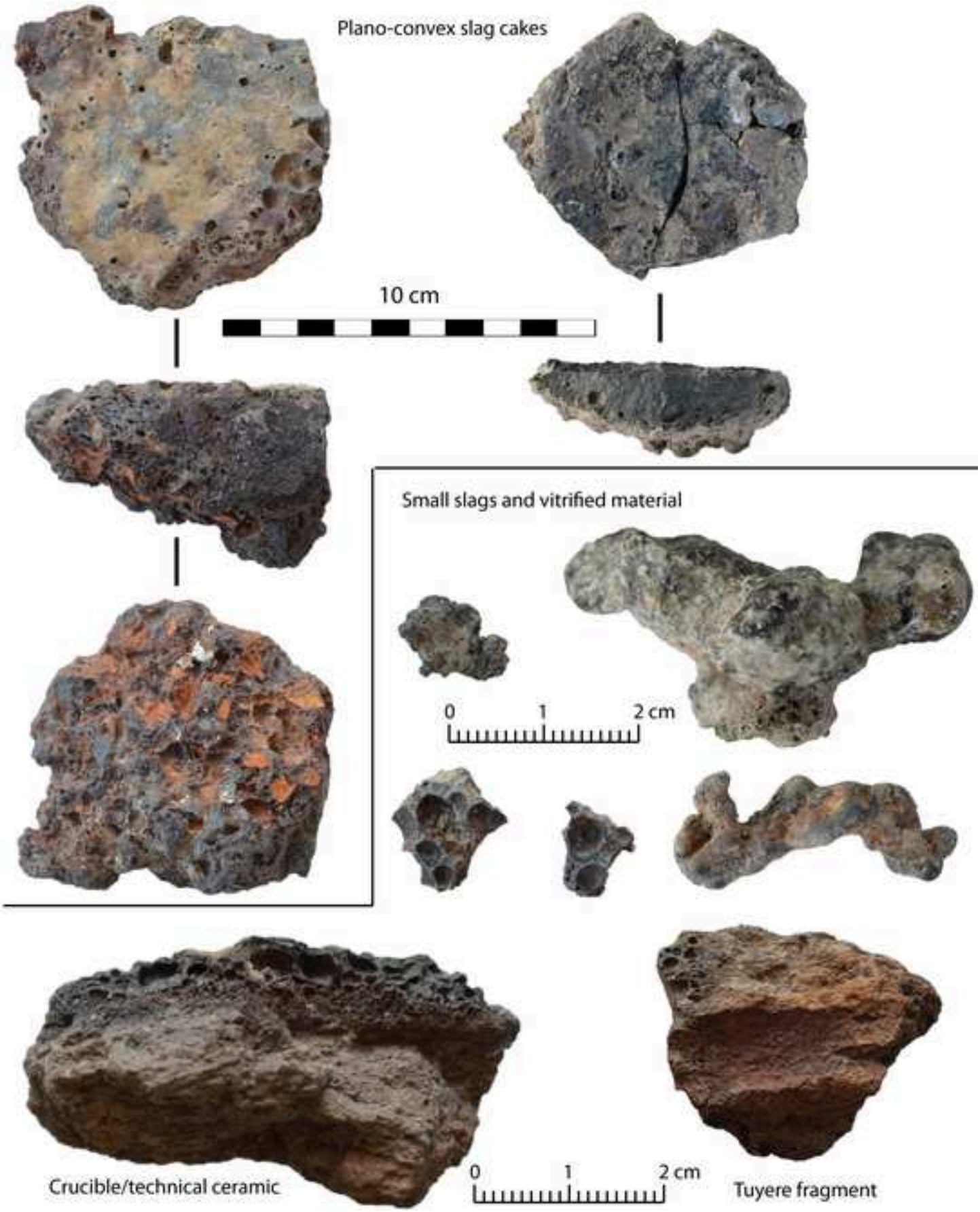

Figure 5

Click here to access/download;Figure;Fig5_MG_StoneAntler.tif

Figure 6

Click here to access/download;Figure;Fig6_SmithingEvidence.tif

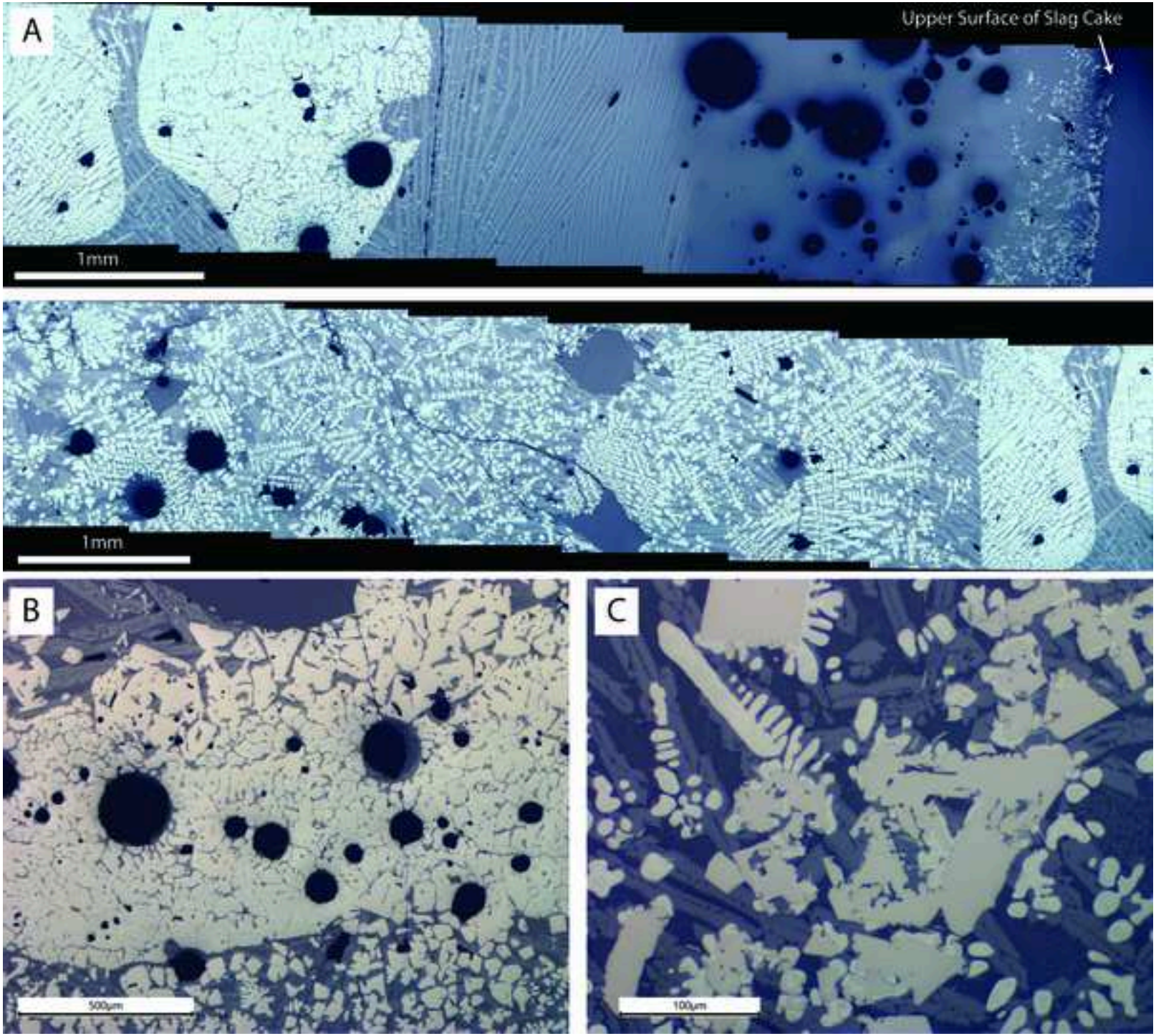

Figure 7

Click here to access/download;Figure;Fig7_MetalParticles.tif

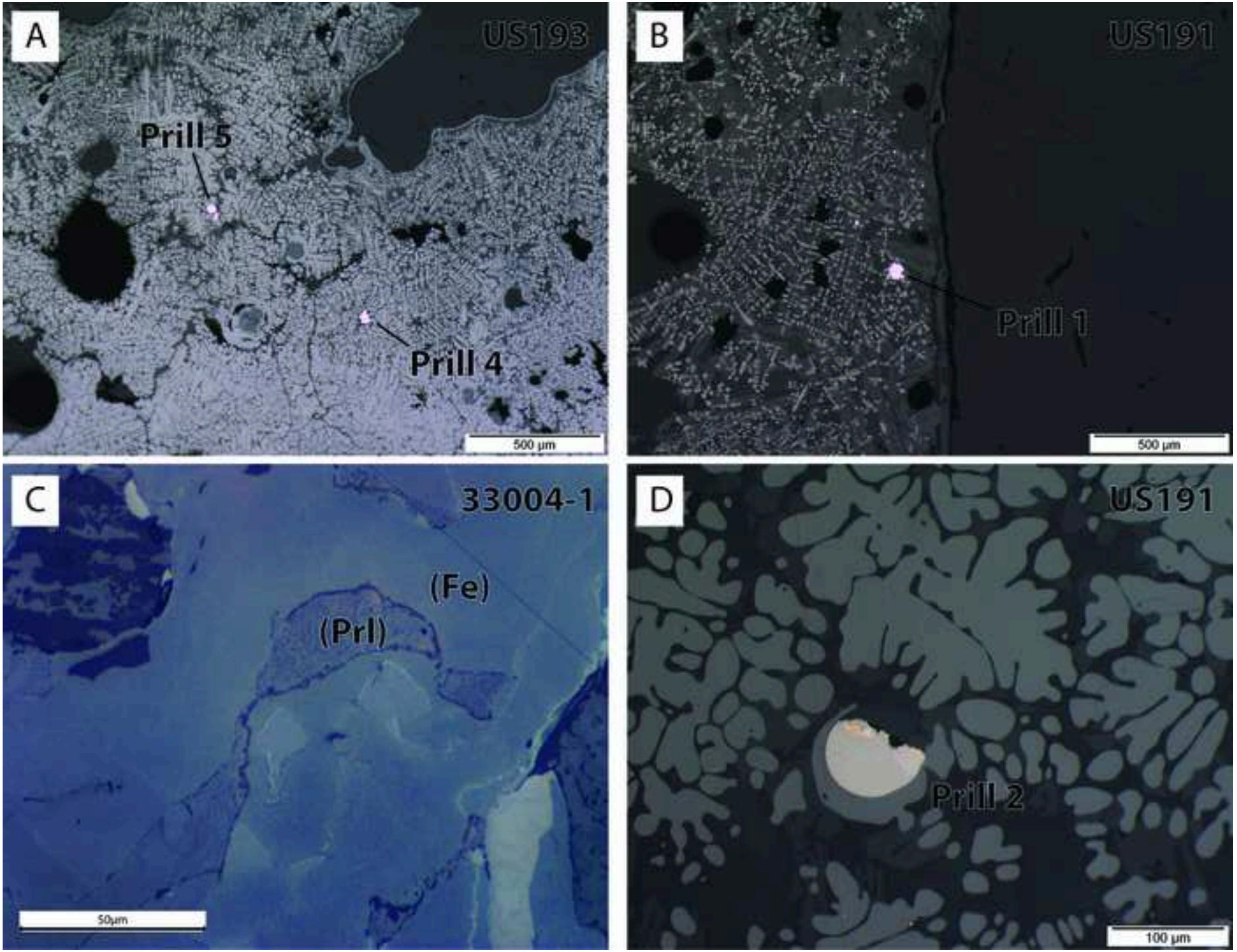

Figure 8

Click here to access/download;Figure;Fig8_VesicularSlags.jpg

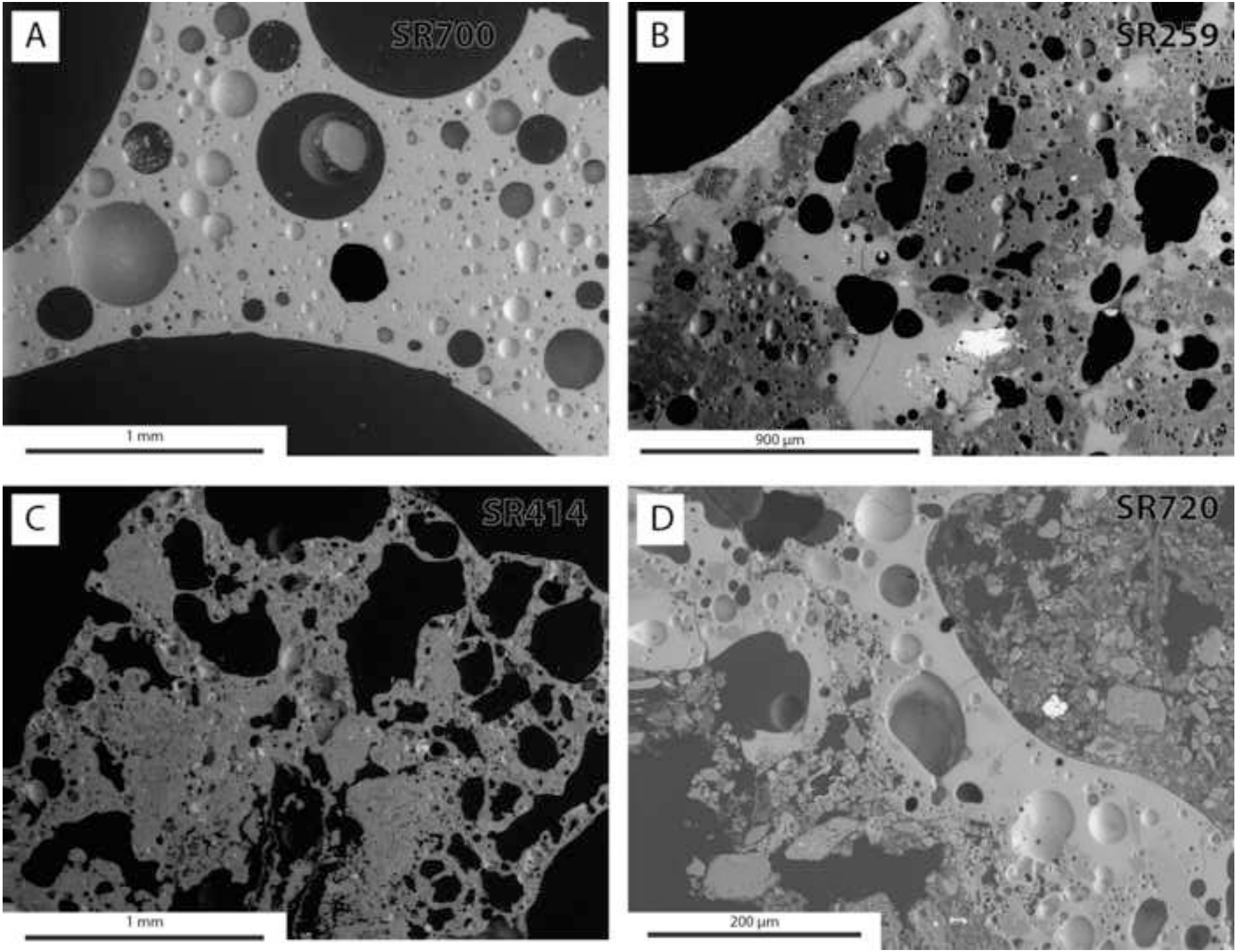

Figure 10

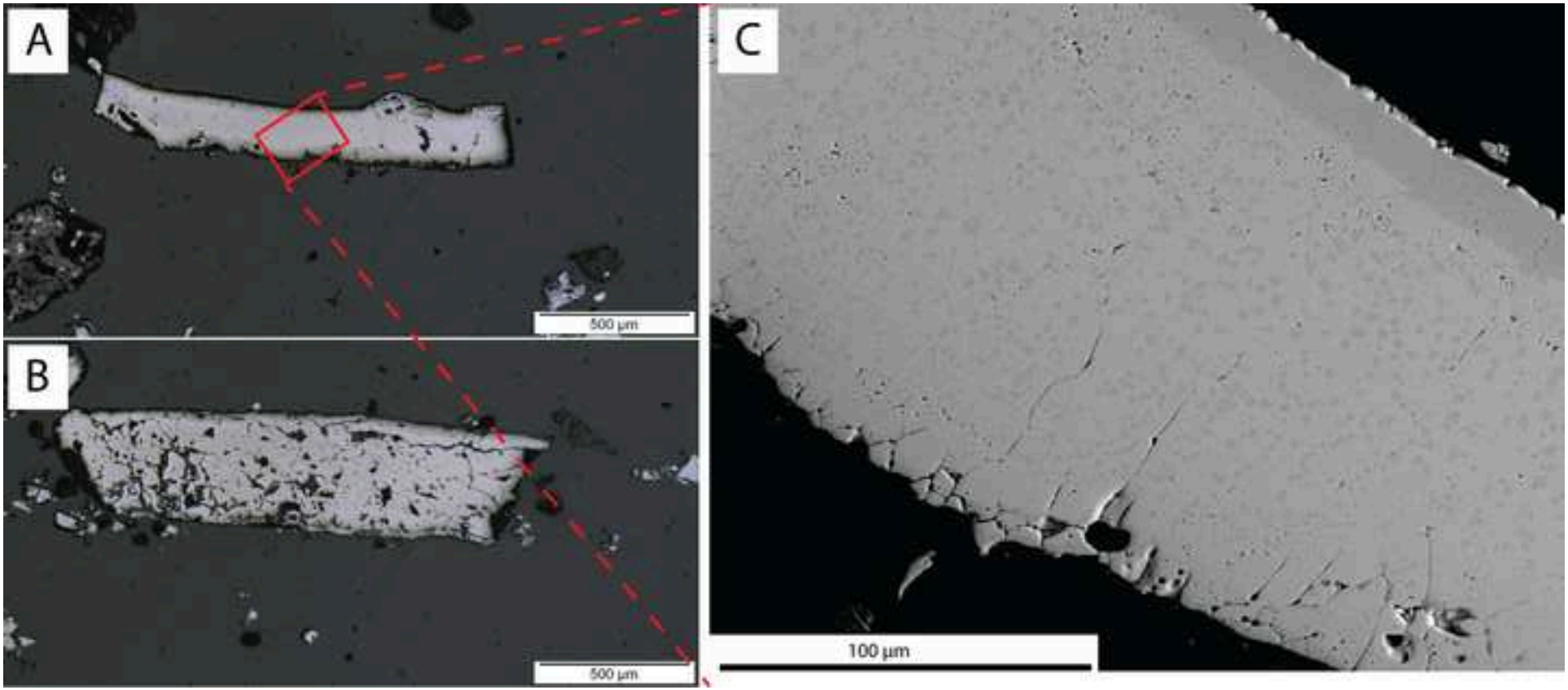

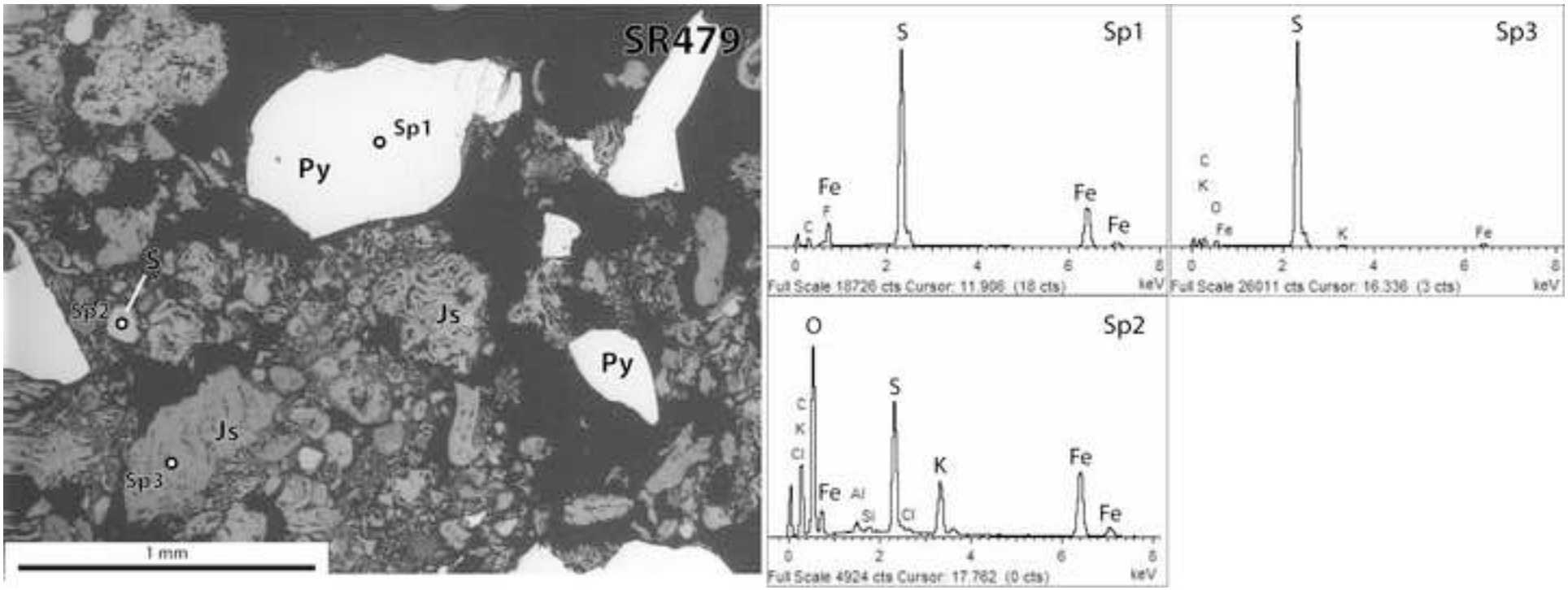

Supplementary data to this article can be found online at https://doi.org/10.1016/j.jas.2020.105220.